

# Properties of Transducers: Underwater Sound Sources and Receivers

Stephen C. Butler  
Sensors and Sonar Systems Department



**Naval Undersea Warfare Center Division  
Newport, Rhode Island**

Approved for public release; distribution is unlimited.

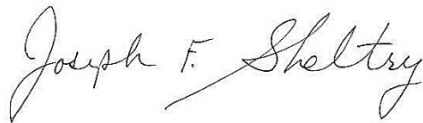
## **PREFACE**

This document was prepared under funding document N0001418WX01584, principal investigator Stephen C. Butler (Code 1535). The sponsoring activity is the Office of Naval Research, program manager Michael J. Wardlaw (ONR-321MS).

The technical reviewer for this report was Richard A. Katz (Code 1552).

The author wishes to thank the staff at NUWCDIVNPT for their help in this document.

**Reviewed and Approved: 19 December 2018**

A handwritten signature in cursive script that reads "Joseph F. Sheltry".

**Joseph F. Sheltry**  
**Head, Sensors and Sonar Systems Department**



REPORT DOCUMENTATION PAGE					Form Approved OMB No. 0704-0188	
<p>The public reporting burden for this collection of information is estimated to average 1 hour per response, including the time for reviewing instructions, searching existing data sources, gathering and maintaining the data needed, and completing and reviewing the collection of information. Send comments regarding this burden estimate or any other aspect of this collection of information, including suggestions for reducing this burden, to Department of Defense, Washington Headquarters Services, Directorate for Information Operations and Reports (0704-0188), 1215 Jefferson Davis Highway, Suite 1204, Arlington, VA 22202-4302. Respondents should be aware that notwithstanding any other provision of law, no person shall be subject to any penalty for failing to comply with a collection of information if it does not display a currently valid OPM control number.</p> <p>PLEASE DO NOT RETURN YOUR FORM TO THE ABOVE ADDRESS.</p>						
1. REPORT DATE (DD-MM-YYYY) 19-12-2018		2. REPORT TYPE Technical Document		3. DATES COVERED (From – To) October-2018 to December-2018		
4. TITLE AND SUBTITLE  Properties of Transducers: Underwater Sound Sources and Receivers					5a. CONTRACT NUMBER	
					5b. GRANT NUMBER	
					5c. PROGRAM ELEMENT NUMBER	
6. AUTHOR(S)  Stephen C. Butler					5. d PROJECT NUMBER	
					5e. TASK NUMBER	
					5f. WORK UNIT NUMBER	
7. PERFORMING ORGANIZATION NAME(S) AND ADDRESS(ES)  Naval Undersea Warfare Center Division 1176 Howell Street Newport, RI 02841-1708					8. PERFORMING ORGANIZATION REPORT NUMBER  TD 12,289	
9. SPONSORING/MONITORING AGENCY NAME(S) AND ADDRESS(ES)  Office of Naval Research 875 North Randolph Street Arlington, VA 22203					10. SPONSORING/MONITOR'S ACRONYM  ONR	
					11. SPONSORING/MONITORING REPORT NUMBER	
12. DISTRIBUTION/AVAILABILITY STATEMENT  Approved for public release; distribution is unlimited.						
13. SUPPLEMENTARY NOTES						
<p><b>14. ABSTRACT:</b> Transducers are used in all aspects of naval sonar systems on surface ships and submarines for target classification and detection, depth and surface sounding, acoustic communication, homing torpedoes, obstacle avoidance, echolocation, and alike. The ability to receive and generate underwater sound is based on the science and art of transducer design, which is a specialized science and technology of its own. A sonar transducer is a device that generates acoustic energy and or receives acoustic energy. Sonar transducers used in the Navy usually consist of arrays of individual transducer elements so that directional beams are formed to send or receive acoustic energy into directions where it is wanted. In many sonar systems the arrays have both a separate transducer for generating sound (projector) and receiving sound (hydrophone), and in some sonar systems the transducer is used as both in order to save weight, space, and cost. An overview of transducers that are used for transmitting sound (projectors) and receiving sound (hydrophones) for underwater sonar applications is presented. Basic sonar transducer design fundamentals are discussed along with working design examples for various projector and hydrophone designs are shown, as well as an extended list of references.</p>						
<p><b>15. SUBJECT TERMS</b> Transducers, Underwater Sound Sources and Receivers; Hydrophone Preamplifiers and Self-Noise; Vector Hydrophones and Sensors; Advanced Transducer Technology, Sonar, Underwater Acoustics</p>						
16. SECURITY CLASSIFICATION OF:			17. LIMITATION OF ABSTRACT  SAR	18. NUMBER OF PAGES  53	19a. NAME OF RESPONSIBLE PERSON Stephen C. Butler	
a. REPORT  U	b. ABSTRACT  U	c. THIS PAGE  U			19b. TELEPHONE NUMBER (Include area code) (401) 832-5101	



## TABLE OF CONTENTS

Section	Page
LIST OF ABBREVIATIONS AND ACRONYMS .....	iii
1 INTRODUCTION .....	1
2 TRANSDUCER FUNDAMENTALS .....	4
2.1 The Projector .....	6
2.2 The Hydrophone .....	18
2.3 Hydrophone Preamplifiers and Self-Noise .....	24
2.4 Vector Hydrophones and Sensors .....	27
2.5 Advanced Transducer Technology .....	39
3 SUMMARY .....	41
4 REFERENCES .....	41

## LIST OF ILLUSTRATIONS

Figure	Page
1 AN/SQS-26 Surface-Ship Sonar System Array .....	2
2 AN/SQS-26 Surface-Ship Transducer Element .....	2
3 AN/BSY-2 Submarine Bow Sonar Array .....	3
4 Submarine LF Hydrophone Element .....	3
5 Submarine WAA Flank Array .....	4
6 An Illustration of the Wide Variety of Available Sizes and Shapes of Piezoelectric Ceramic Elements .....	5
7 Tonpilz Transducer .....	6
8 Transducer Transmit Equivalent Circuit Model .....	7
9 Radiation Impedances: $R_{\text{rad}}$ and $X_{\text{rad}}$ .....	8
10 Transducer Input Impedance Magnitude .....	10
11 Transducer Transmitting Voltage Response .....	11
12 USRD J9 Moving Coil Projector .....	12
13 Typical TVR and TCR for USRD Type J9 Transducer .....	12
14 Flooded Ring Transducer .....	13
15 Example of Measured Transmitting Voltage Response of a FFR .....	13
16 Flextensional Transducer and Photograph .....	14
17 Transmitting Voltage Response of Flextensional Transducer .....	14
18 Hydroacoustic Transducer and Photograph .....	15
19 Typical Transmitting Response for Hydroacoustic Transducer .....	15
20 Air Gun Impulsive Underwater Transducer and Photograph .....	16
21 Energy Source Level Response as a Function of Fundamental Frequency for Three Different Air Guns .....	17

## LIST OF ILLUSTRATIONS (Cont'd)

Figure	Page
22	A Standard U.S. Navy Explosive Sound Signal .....17
23	Pressure Waveform from the Explosion of a 0.82-kg SUS Charge at 102-m and Source Level Measurements in 1/3 Octave Bands for 0.82-kg SUS Charges at 23.5-m, 99.6-m, and 194.4-m .....18
24	Transducer Receiving Equivalent Circuit Model .....19
25	Transducer Receiving Voltage Sensitivity Response .....20
26	Capped Cylinder Hydrophone .....21
27	Equivalent Circuit of a Hydrophone .....22
28	Circuit of a Hydrophone Further Reduced.....22
29	The F42 Transducers.....23
30	Typical FFVS for the F42 Transducers .....24
31	Measurement Hydrophone, Dimensions in Centimeters .....26
32	Typical Open-Circuit FFVS of USRD Type H56 Hydrophone at End of 23-m Cable .....26
33	Noise Voltage at Input of USRD Low-Noise Amplifier for H56 Hydrophone, 100-pF Source .....27
34	Equivalent Noise Pressure Level of H56 Hydrophone Compared with the Noise Level of Sea State Zero .....27
35	Vector Sensor Beam Pattern Types .....28
36	The Dipole Sensors, Two Out-of-Phase Omni Sensors Spaced $d \leq \lambda/2$ .....29
37	The Cardioid Sensor .....29
38	The Relative Spherical Wave Pressure and Velocity as a Function of Range and Wavelength .....30
39	Ceramic Vane Pressure Gradient Hydrophone .....31
40	Geophone Acoustic Motion Sensor .....32
41	Two-Axis Dipole Hydrophone .....33
42	Measured Acoustic Sensitivity and Beam Pattern of Geophone .....33
43	Single-Axis Acoustic Motion (Velocity) Sensor .....34
44	Flexural Disk Acceleration Sensitivity Response in dB re 1V/g.....35
45	Measured Receive Sensitivity.....35
46	Measured Beam Patterns at 1 kHz .....36
47	Wilcoxon Vector Sensor .....36
48	(a) Hydrophone and (b) Accelerometer RVS Responses Along the X, Y, and Z Axis .....37
49	(a) Hydrophone and Accelerometer Beam Patterns Along the (b) X and Y Axis and (c) Z Axis at 7-kHz .....37
50	Multimode Hydrophone Ceramic Cylinders Electroded into Quadrants.....38
51	Multimode Hydrophone Example.....39
52	Configuration of Piezo-Rubber (Left) and 1-3 Composite (Right) Material.....40
53	Mandrel Fiber-Optic Acoustic Sensor .....40
54	The Fiber-Optic Interferometer Hydrophone Technique.....41

## LIST OF ABBREVIATIONS AND ACRONYMS

ADP	Ammonium Dihydrogen Phosphate
BaTiO <sub>3</sub>	Barium Titanate
BB	Bottom Bounce
CZ	Convergence Zone
dB	Decibel
DI	Directivity Index
DICASS	Directional Command Activated Sonobuoy System
DIFAR	Directional Frequency Analysis and Recording (Ranging)
Dm	Mean Diameter
EDO	EDO Corporation, Salt Lake City, UT
FEA	Finite Element Analysis
FFR	Free Flooded Ring
FFVS	Free-Field Voltage Sensitivity
ID	Inside Diameter
LF	Low-Frequency
NDRC	National Defense Research Committee
NUSC	Naval Underwater Systems Center
NUWC	Naval Undersea Warfare Center
OD	Outside Diameter
PIN-PMN-PT	Lead Indium Niobate-Lead Magnesium Niobate-Lead Titanate
PMN-PT	Lead Magnesium Niobate-Lead Titanate
PVDF	Poly Vinylidene Flouride
PZR	Piezo-Rubber
PZT	Lead Zirconate Titanate
rms	Root-Mean-Square
R <sub>rad</sub>	Resistance Radiation Impedance
RVS	Receive Voltage Sensitivity
SL	Source Level
SSN	Submarine, Fast Attack, Nuclear Propulsion
SUS	Signal, Underwater Sound
TCR	Transmitting Current Response
TNT	Trinitrotoluene
TVR	Transmitting Voltage Response
USRD	Underwater Sound Reference Detachment (Orlando, FL)
WAA	Wide Aperture Array
X <sub>rad</sub>	Reactance Radiation Impedance
Z <sub>rad</sub>	Radiation Impedance Magnitude





# **PROPERTIES OF TRANSDUCERS: UNDERWATER SOUND SOURCES AND RECEIVERS**

## **1. INTRODUCTION**

Most sonar systems utilize some form of transducer to generate acoustic energy or to receive acoustic energy. Sonar transducers normally, but not always, generate or receive sound through a process of converting electric energy. They usually consist of arrays of individual transducer elements, by means of which a directional beam is formed to send or receive acoustic energy into directions where it is wanted. In many sonar systems the arrays have both a separate transducer for generating sound (projector) and receiving sound (hydrophone), and in some sonar systems the transducer is used both as a projector or a hydrophone in order to save weight, space, and cost.

An example of this is shown in figure 1 for the hull bow mounted surface ship AN/SQS-26 sonar system used in echo-ranging.<sup>1</sup> The AN/SQS-26 transducer array weighs 60,000 lb, has 72 vertical staves with 8 transducer elements per staff and is about 16-ft in diameter and 5-ft in height. The transducer element shown in figure 2 is approximately 27-inches in length with a radiating face (head mass), and is used as both a transmitter (projector) and receiver. This scanning sonar has the capabilities of direct path range, bottom bounce (BB) reflected and convergence zone (CZ) propagation.<sup>2 and 3</sup> The AN/SQS-26 sonar system was a U.S. Navy surface ship, bow-mounted, active/passive sonar developed by the Naval Underwater Systems Center (NUSC) (now the Naval Undersea Warfare Center (NUWC) Division, Newport, RI) and built by General Electric and the EDO Corporation (EDO) and used from the 1960's through the 1970's.<sup>4 and 5</sup>

An example of a Navy sonar system that has separate transducers for generating sound (projector) and receiving sound (hydrophone) is the USS *Seawolf* (SSN 21)-class submarine Hull AN/BSY-2 Sonar Array system shown in figure 3.<sup>6</sup> The AN/BQQ-5D sonar suite is the major system component within the AN/BSY-2 Sonar Array system which includes the large passive bow spherical array, the low-frequency (LF) conformal bow array and the active hemispherical transmit array.<sup>2 and 7</sup> The large passive bow spherical array is 24-feet in diameter which consists of only hydrophones and supplemented by a LF conformal passive bow array. A LF conformal array hydrophone element is shown in figure 4. This hydrophone has two Lead Zirconate Titanate (PZT) ceramic cylinders mounted end-to-end that are encapsulated in a neoprene rubber jacket and are used strictly for passive listening. The active only hemispherical transmit array is a 15-ft diameter half sphere with only projectors. The submarine is also outfitted with planar flank arrays mounted along the port and starboard side of the submarine's hull, known as the wide aperture array (WAA). The submarine WAA Flank array is shown in figure 5.<sup>1, 4, 7, and 8</sup>

The ability to receive and generate underwater sound is based on the science and art of transducer design. It is a specialized science and technology of its own, which will be described in the next section in more detail. The interested reader may find the basic principles and more in-depth theory of electroacoustic transduction in references 9 through 12. The design and construction of actual transducers are well described in two volumes of the National Defense Research Committee (NDRC) Summary Technical Reports (reference 13). Not all projectors are

electroacoustic. Explosive charges, for example, when detonated in water convert chemical energy into sound energy with interesting acoustical properties, which will be described later.

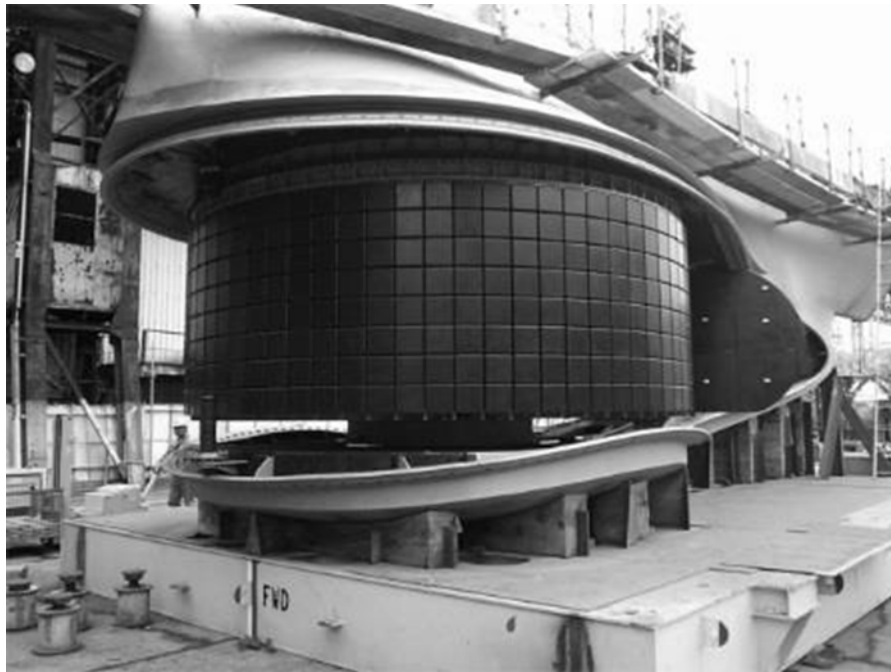


*Figure 1. AN/SQS-26 Surface-Ship Sonar System Array<sup>1</sup>*

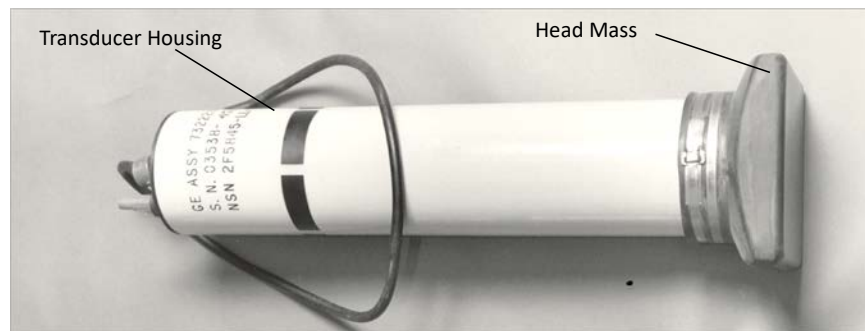


*Figure 2. AN/SQS-26 Surface-Ship Transducer Element<sup>12</sup>*

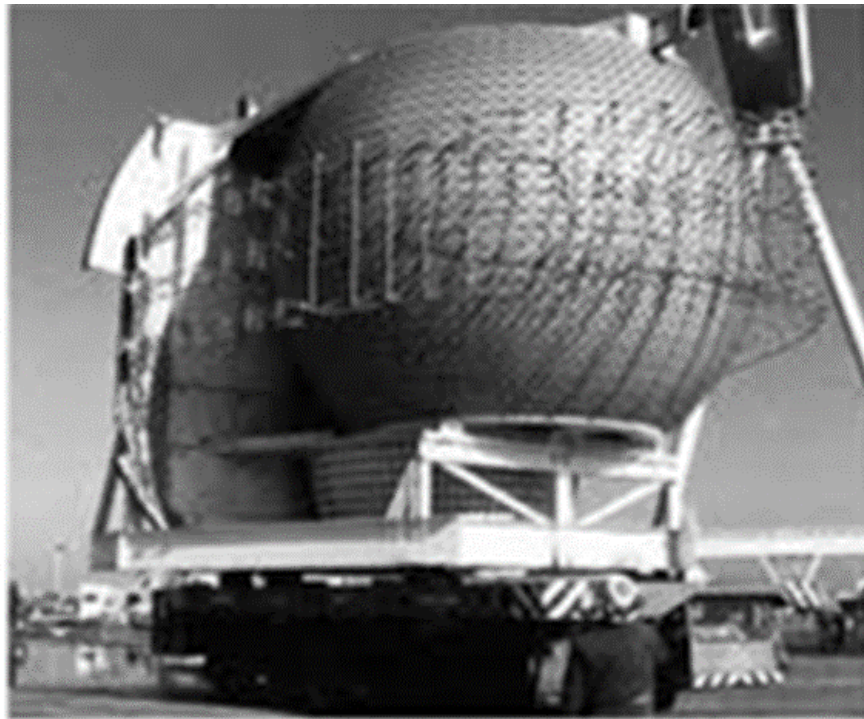


*Figure 3. AN/BSY-2 Submarine Bow Sonar Array<sup>6 and 7</sup>*



*Figure 4. Submarine LF Hydrophone Element*

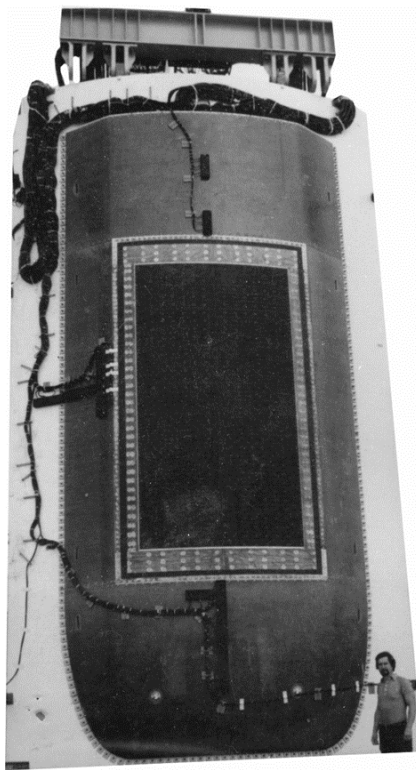


*Figure 5. Submarine WAA Flank Array<sup>1</sup>*

## 2. TRANSDUCER FUNDAMENTALS

A transducer is a device that converts one form of energy to another form of energy. A sonar transducer is a reciprocal device that receives and transmits acoustical energy (sound waves). A transducer that transmits underwater acoustical sound waves is called a sound projector and is analogous to an audio loudspeaker that transmits in air. A transducer that receives acoustical sound waves is called a hydrophone and is analogous to a microphone. Some transducers in the Navy both transmit and receive, as in echolocation systems. The main active materials in a sonar transducer are piezoelectric ceramics, where piezo is Greek for pressure, i.e., pressure-electric. That is, when a mechanical stress (pressure) is applied to the piezoelectric ceramic, an electric field or charge is developed across the element known as the direct piezoelectric effect. The piezoelectric effect is a reciprocal quantity in that when an electric field is applied, it will generate a mechanical strain in the piezoelectric ceramic and this is referred to as the inverse-piezoelectric effect.

The piezoelectric effect was first demonstrated with Quartz in 1880 by French physicist brothers Jacques and Pierre Currie. Quartz crystals are naturally piezoelectric and were used on many post-WW I and WW II sonar systems. Some other crystalline naturally piezoelectric substances also used during this time and later, are Rochelle salt and Ammonium Dihydrogen Phosphate (ADP).<sup>13 and 14</sup> During the 1940's and 1950's the USA, Russia, and Japan discovered a new class of manmade synthetic piezoelectric materials called ferroelectrics, which exhibited

piezoelectric constants much higher than Quartz crystals. This led to intense research to develop Barium Titanate ( $\text{BaTiO}_3$ ) and later PZT materials, which are used in the majority of all Navy sonar transducers.<sup>15 and 16</sup> Piezoelectric PZT ceramics can be formed in many different shapes including bars, plates, rings, discs, cylinders, hemi-spheres, and spheres making them the ideal choice for sonar transducer applications. The different shapes are formed from piezoelectric ceramic powder which is mixed as a slurry, poured into molds, sintered at high temperatures, milled to exact dimensions, silvered on the ends or inner and outer surfaces, and then polarized.

There are three commonly used PZT type materials used in the manufacture of Navy sonar transducers, which are U. S. Navy Type I, II, and III.<sup>17</sup> Navy Type I (PZT-4) is a hard piezoelectric material. The “hard” refers to it being hard to electrically and thermally depolarize. Navy Type I has material properties that are suited for active projectors, passive hydrophones, or transducers that do both these functions. Navy Type II (PZT-5) is a soft piezoelectric material. The “soft” refers to it being easier to depolarize, and has material properties that are more suited for hydrophones. Navy Type III (PZT-8) is a hard piezoelectric material and has properties more suited for high-power projectors due to low electrical and mechanical losses. A complete list of material properties of Navy types can be found in references 10 and 18. An illustration of the wide variety of available sizes and shapes of piezoelectric ceramics are shown in figure 6.



***Figure 6. An Illustration of the Wide Variety of Available Sizes and Shapes of Piezoelectric Ceramic Elements (Included in this photograph are plates, bars, rings (both radially and circumferentially polarized), spheres, and small composite vibrators.)<sup>10</sup>***

The Navy is currently investing in a new family of synthetic piezoelectric materials known as signal crystals, which exhibit more active piezoelectric constants and higher strains than PZT's.

These include Lead Magnesium Niobate-Lead Titanate (PMN-PT) and Lead Indium Niobate-Lead Magnesium Niobate-Lead Titanate (PIN-PMN-PT) and show great promise in current and future transducer design.<sup>11</sup> Other active transducer materials exhibit magnetostriction such as Nickle (references 13 and 19) and Terfenol-D which have strains 5-to-10 times greater than PZT's.<sup>20</sup>

## 2.1 THE PROJECTOR

Most sonar transducer projectors in use today use a stack of piezoelectric ceramic rings or cylinders as the active vibrating element. The basic components of a typical transmitting transducer are a head mass, tail mass, an active element "PZT", a waterproof housing "case", tuning/matching transformer, and an electrical cable, as shown in figure 7.<sup>21</sup> This is a typical ceramic longitudinal transducer and commonly known as a "Tonpilz" type transducer, which is German for the words "sound mushroom" due to its physical appearance. A Tonpilz longitudinal type transducer is generally made up of three major parts; a ceramic ring stack sandwiched between two masses, the tail mass, and head mass. The ceramic ring stack is typically composed of many piezoelectric ceramic rings epoxied together mechanically in series and electrically connected in parallel. When an electrical sinusoidal voltage signal is applied to this ceramic stack, the stack will expand and contract longitudinally, and radiate into the medium from the surface of the head mass.

The tail mass is usually made of a heavy material such as steel or tungsten and the head mass is usually made of light stiff material such as aluminum or magnesium. A mechanical stress bias is necessary for high-power operation and is applied to the piezoceramic stack by means of a stress rod or bolt running longitudinally through the assembly. The stress rod keeps the ceramic element under constant compressional stress; thus, preventing the ceramic from going into tension and fracturing under high-drive conditions, due to its low-tensile strength. The collar shown in figure 7 is a metal stand-off between head mass and ceramic stack. The tuning ring is typically a fiberglass ring used to adjust the final resonance of the transducer by choosing different ring thicknesses. The compliant retainer ring mounts the tail mass to the housing. Both the head mass and part of the housing are rubber molded for waterproofing.

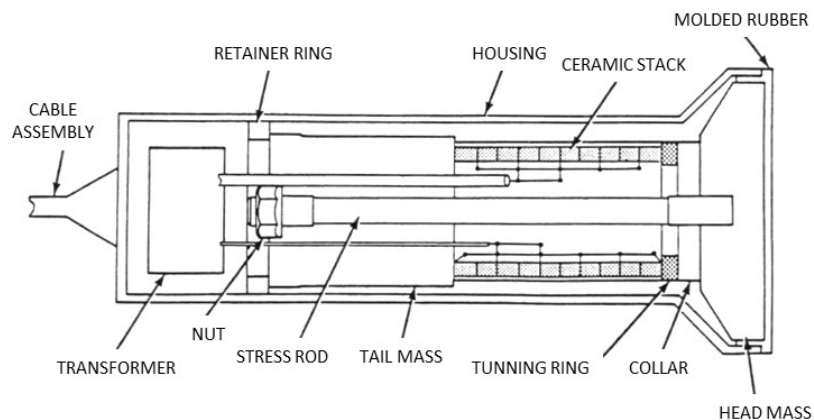


*Figure 7. Tonpilz Transducer<sup>21</sup>*

A sonar transducer is an electromechanical vibrating oscillator that has a mass, spring, and damping (i.e., dashpot) associated with it. In the case of a PZT ceramic cylinder or ring, the mass portion of the ceramic is associated with its dimension and density of the material, the spring is associated with the elastic modulus of the active material, and the damping is associated with its mechanical losses. In the case of a piston “Tonpilz” type transducer, the mass would be the piston or head mass, the spring would be the compliance of the PZT ceramic stack, and the damping would be mechanical losses of the transducer. The tail mass, if heavy enough, could be treated as a rigid mount; otherwise, a lighter tail mass would need to be included making it a Mass-Spring-Mass two degrees-of-freedom system. In order to analyze such a mechanical vibration system, one would solve the system of equations of motion for a mass-spring-damped system or employ equivalent circuit modeling approaches that use mechanical-to-electrical analogues, where Force is Voltage, Velocity is Current, Mass is Inductance, Spring Stiffness  $K$  is  $1/\text{Capacitance}$ , and Dashpot (Damper) is Resistance. Thus, one can solve a mechanical problem as if it were an electrical circuit using network circuit theory.<sup>22</sup> Finite element modeling allows an alternative accurate approach for more complicated transducer designs.<sup>23</sup>

The electroacoustic transducer equivalent electrical circuit used to describe its behavior can be represented by a simplified generalized equivalent circuit shown in figure 8, which is valid in the vicinity of the transducer resonance. Such a circuit is made up of three parts: (1) the electrical impedance section, (2) the mechanical impedance section, and (3) the acoustical radiation section. The electrical impedance section is composed of the dielectric electrical losses,  $R_o$ , blocked or clamped capacitance,  $C_o$ , associated with the ceramic stack, and an idealized electro-mechanical transformer ( $1:\phi$ ) that converts the drive voltage into a mechanical force,  $F$ . The mechanical impedance section is composed of: the head mass,  $m_h$ ; tail mass,  $M_t$ ; mechanical losses,  $R_l$ ; and stiffness or compliance,  $C_c$ , of the ceramic stack along with the head mass velocity,  $v$ .

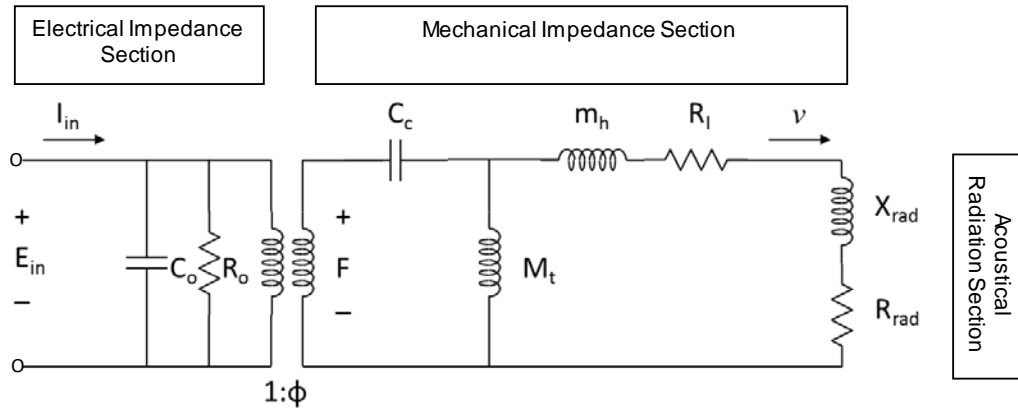


**Figure 8. Transducer Transmit Equivalent Circuit Model**

The acoustical impedance is the load impedance exerted by the medium (water) on the radiating face of the head mass. This acoustical load impedance is referred to as radiation impedance ( $Z_{rad}$ ) and is a frequency-dependent quantity containing resistive Resistance Radiation Impedance ( $R_{rad}$ ) and mass reactance Reactance Radiation Impedance ( $X_{rad}$ ) elements and expressed as,

$$Z_{rad} = R_{rad} + jX_{rad} = \rho_w c_w A_p (R_1(x) + jX_1(x)),$$

where  $\rho_w$  and  $c_w$  are, respectively, the density and sound speed of the fluid (water), and where  $A_p$  is the piston surface area,  $\pi a_p^2$ , and  $a_p$  is the piston radius. For the case of a circular piston in a rigid baffle the piston resistance function  $R_1(x)$  is governed by the first-order Bessel function,  $J_1(x)$ , and piston reactance function  $X_1(x)$ , is governed by the first-order Struve function,  $H_1(x)$ , which acts like a mass of fluid. Here

$$R_1(x) = 1 - 2J_1(x)/x \text{ and } X_1(x) = 2H_1(x)/x,$$

where  $x = 2ka_p$  and  $k$  is the wavenumber  $\omega/c_w$ . The values of these radiation impedances versus  $x/2 = ka_p$  (wave number times piston radius) are plotted in figure 9, for a circular piston of radius,  $a_p$ , in an infinite rigid baffle.<sup>24</sup> The values have been normalized by the characteristic impedance “ $\rho_w c_w A_p$ ”.

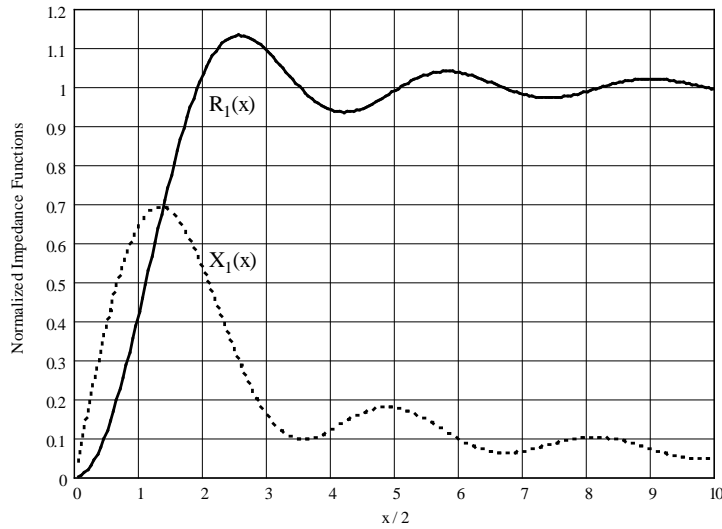


**Figure 9. Radiation Impedances:  $R_{rad}$  and  $X_{rad}$**

The curves show that when  $ka \ll 1$ ; that is, where the piston is small compared to acoustic wavelength ( $D < \lambda$ ), the radiation impedance is mostly mass reactance ( $X_{rad}/\omega$ ). This mass will add to the head mass, lowering the transducer's resonance frequency. The radiation resistance in this region of  $ka$  is low in value making the transducer an inefficient projector, since the radiated acoustic output power is given by  $v^2 R_{rad}$ , where “ $v$ ” is the velocity of the piston. On the other hand, when  $ka > 2$ ,  $D > \lambda$  the mass reactance approaches zero and the radiation resistance approaches unity ( $R_{rad} = 1$ ), or un-normalized “ $\rho c A_p$ ”. In this region the transducer load is a pure real resistance as a function of frequency. A maximum amount of acoustic power is radiated in this region for a given velocity  $v$ . Dividing the input drive voltage,  $E_{in}$ , by the input drive current,  $I_{in}$ , is the electromechanical or electroacoustical complex input impedance,  $Z_{in}$ , of the transducer.



As an example, the design of a Tonpilz Navy transducer used as both a transmitter and receiver in the 5-kHz AN/SQS-23 surface ship sonar system (references 2, 3, 10, and 15) has an aluminum head mass that is 1.4-kg with a 14-cm diameter radiating surface, a steel tail mass that is 2.6-kg and four PZT-4 ceramic rings that operate in their thickness mode with an outer diameter of 59.7-mm, inner diameter of 48-mm, and thickness of 15.7-mm each. The stress rod is typically significantly more compliant than the ceramic stack and will be ignored for this example. This transducer also has a tuning or matching transformer wired across the ceramic stack which will also be ignored in this example. In the equivalent circuit model, the electromechanical turns ratio  $\emptyset$  and blocked capacitance  $C_o$  are both functions of the piezoelectric material properties, which are  $\emptyset = A_c d_{33} / s_{33}^E t$ ,  $C_o = C_f (1 - k_{33}^2)$ ,  $C_f = A_c K_{33}^T \epsilon_o n / t$ ,  $R_o = (2\pi f C_f \tan \delta)^{-1}$  and ceramic compliance is given by  $C_c = s_{33}^E t n / A_c$ , where  $d_{33}$  is the piezoelectric strain constant ( $285 \times 10^{-12}$  m/V for PZT-4),  $s_{33}^E$  is the short-circuit piezoelectric elastic constant ( $15 \times 10^{-12}$  m<sup>2</sup>/N for PZT-4),  $k_{33}$  is the piezoelectric coupling coefficient (0.7 for PZT-4),  $K^T$  is the free piezoelectric dielectric constant (1,300 for PZT-4),  $\epsilon_o$  is permittivity of free space,  $A_c$  is the cross-sectional area of the piezoelectric ring,  $t$  is the thickness of a piezoelectric ring,  $n$  is the number of the piezoelectric rings, and  $\tan \delta$  is the dielectric loss tangent (0.01 typical for PZT-4). The calculated equivalent circuit values are:  $\emptyset$  is 1.2,  $C_f$  is 2.9-nF,  $C_o$  is 1.48-nF,  $R_o$  is 5.5-Meg-ohms at 1-kHz,  $R_l$  is 4,000 ohms, and  $C_c$  is  $9.6 \times 10^{-10}$ -m/N. With,  $m_h$ , and,  $M_t$ , one can calculate the fundamental resonance,  $f_r$ , for a mass-spring-mass system without the water load by,

$$f_r = 1/2\pi \sqrt{\left(1/(C_c m_h)\right) \left(1 + m_h/M_t\right)},$$

and this gives a resonant frequency of 5.4-kHz.

The electrical input impedance ( $E_{in}/I_{in}$ ) of a sonar transducer is an important quantity, as it is related to the amount of electrical power that is needed to produce an acoustic pressure and since a transducer is a coupled electromechanical device the resonant frequencies are displayed within its response. A complex impedance response can also determine the stability of the transducer from its shape of the response. For example, if the response deviates from its original response the transducer may have been damaged. The solved equivalent electrical circuit input impedance magnitude for this transducer example is shown in figure 10 with and without a water load. The no water load case would be similar to a transducer measured in-air, and for that case the radiation impedances  $R_{rad}$  and  $X_{rad}$  values are short circuited. For the water-loaded case, radiation impedances  $R_{rad}$  and  $X_{rad}$  load values are included in the circuit model. The impedance response shows both its resonance  $f_r$  (frequency of minimum impedance) and anti-resonance  $f_a$  (frequency of maximum impedance). The impedance case shows the effect of the radiation impedances, more specifically, the mass load of the radiation reactance,  $X_{rad}$ , which lowers both the resonance frequency values and the radiation resistance,  $R_{rad}$ , which smooths the magnitude levels. Although the electrical input impedance,  $Z_{in}$ , of a transducer is important for the power amplifier and system design, it is common for transducer designers to use the electrical input admittance  $Y_{in} = I/Z_{in} = G + jB$ , where  $G$  is the conductance and  $B$  is the susceptance. From in-air and in-water admittance data, the input power  $W_{in}$ , the electroacoustic efficiency  $\eta_{ea}$ , mechanical quality factor  $Q_m$ , electrical quality factor  $Q_e$ , and effective coupling coefficient  $k_{eff}$  can be directly calculated, which characterizes the transducer equivalent circuit values and performance parameters.<sup>11 and 12</sup>

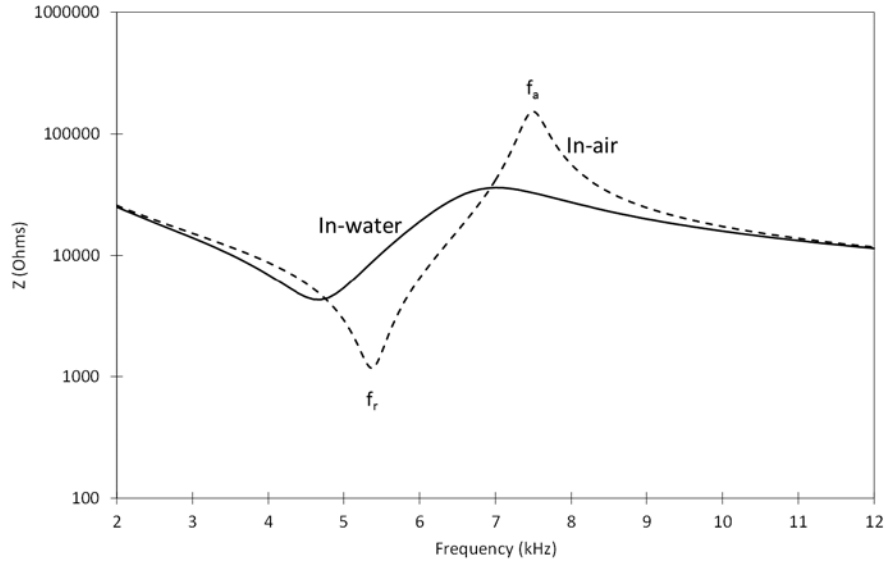


**Figure 10. Transducer Input Impedance Magnitude**

The transmitting voltage response (TVR) is another important transducer quantity or parameter that describes the sonar transducers operation or function. The transmitting response

$$S = p_{out} / E_{in} \cdot d$$

is the on-axis radiated acoustic pressure output,  $p_{out}$ , that a transducer produces due to an applied voltage input,  $E_{in}$ , at a distance,  $d$ . The applied voltage and farfield distance could be any values as long as they are referenced back to 1-volt,  $E_{in}=1$ , and 1-meter,  $d=1$ . In underwater acoustics the “microPascal” ( $p_o = 1 \mu Pa$ ) is used as the standard sound pressure reference unit instead of Pascals and the decibel (dB) is the standard unit used for pressure and intensity quantities. Therefore, the TVR is expressed as,

$$TVR(\text{dB re } 1\mu Pa/V \text{ at } 1 \text{ meter}) = 20 \log S = 20 \log (p_{out} / E_{in} \cdot d) .$$

The transmitting current response (TCR) or TIR is another common quantity or parameter that describes the sonar transducer operation or function. The TCR is the on-axis radiated acoustic pressure of the transducer for 1-ampere applied to the transducer input terminals when at a meter distance from its radiating surface. The TCR is described as the units of decibels relative to 1-micropascal per amp at the reference distance of 1-meter (dB re  $1\mu Pa/\text{amp}$  at 1-meter). The relationship between TIR and TVR is a function of the projectors impedance magnitude and is given by  $TIR = TVR + 20\log|Z_{in}|$ . The radiated acoustic pressure,  $p$ , can be predicted from the velocity,  $v$ , flowing through the radiation impedance in the equivalent electrical circuit (figure 7) by  $P = \rho_w f A_p v / r$  where  $A_p$  is the radiating piston surface area;  $\rho_w$  is the water density;  $f$  is the frequency in Hz; and  $r$  is the distance from the piston. Dividing the radiated acoustic pressure by  $p_o = 1 \mu Pa$ , (sound pressure reference for water) and taking  $20 \log$  of  $p/p_o$  gives the TVR for 1-volt ( $E_{in}=1$ ) and for distance  $r$  of 1-meter. The predicted TVR of the element is shown in figure 11, the peak level in the TVR happens at resonance,  $f_r$ , where the impedance is a minimum.

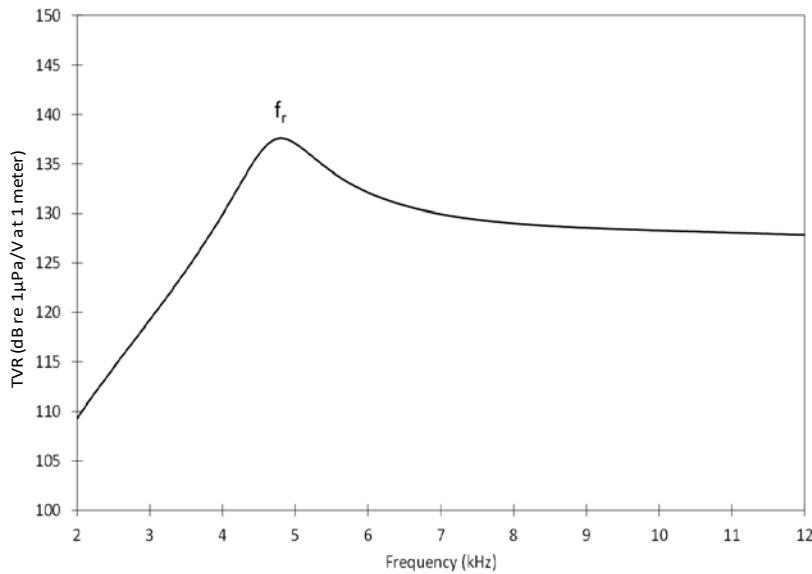


**Figure 11. Transducer Transmitting Voltage Response**

The transducer source level (SL) can be predicted by applying different drive voltage levels in for  $E_{in}$  of equivalent circuit or by adding the drive voltage level in dB to the TVR level as expressed by  $SL = TVR + 20 \log(E_{in})$ . For an example applying a 1,000-V<sub>rms</sub> drive at 5-kHz would produce a source level of 197-dB re 1-μPa at 1-meter or 60-dB more than its TVR level of 137-dB re 1-μPa/V at 1-meter, as shown in figure 10. In rare cases when the older reference distance of 1-yd is still used, a correction factor of 0.78 dB (i.e.  $20 \log 39.4/36$ ) is required to convert the source level reference at 1-meter for the sonar equations that are still expressed in yards. As an example, a projector with a source level of 200-dB re 1-μPa at 1-meter would correspond to a source level of 200.78-dB re 1-μPa at 1-yard.

There are other types of projectors or sound sources that operate on the similar principals as discussed for the Tonpilz Piston transducer as a resonant system, but with different electromechanical driver, mass, and spring mechanisms. Also, there are other types that use non-traditional transduction means (mechanism) to produce sound that will be briefly discussed. The NUWC Underwater Sound Reference Detachment (USRD) Newport, RI, Type J9 transducer laboratory standard underwater sound projector, is shown in figure 12. The J9 projector has a moving coil, (item 12 in figure 12), and is similar to an audio moving coil loudspeaker; however, instead of a paper cone diaphragm, the diaphragm is a stiff but lightweight magnesium diaphragm, (item 9 in figure 12), that is supported by a rubber, (item 1 in figure 12), suspension system that permits large linear movement. In order for the diaphragm not to undergo any static displacement, the projector has a passive pressure compensation rubber bag, (item 15 in figure 12), that equalizes the internal air pressure, (item 14 in figure 12), to that of the external hydrostatic water pressure due to depth. It has a highly damped resonance below 200-Hz and operates from 40-Hz-to-20-kHz as illustrated in its TVR and TCR responses as shown in figure 13. The magnet, (item 4 in figure 12), front pole piece, (item 11 in figure 12), and back pole piece, (item 13 in figure 12), are shown in figure 12. This is a standard projector that can be rented as part of the U.S. Navy's NUWC USRD standard loan transducer program.<sup>25</sup>

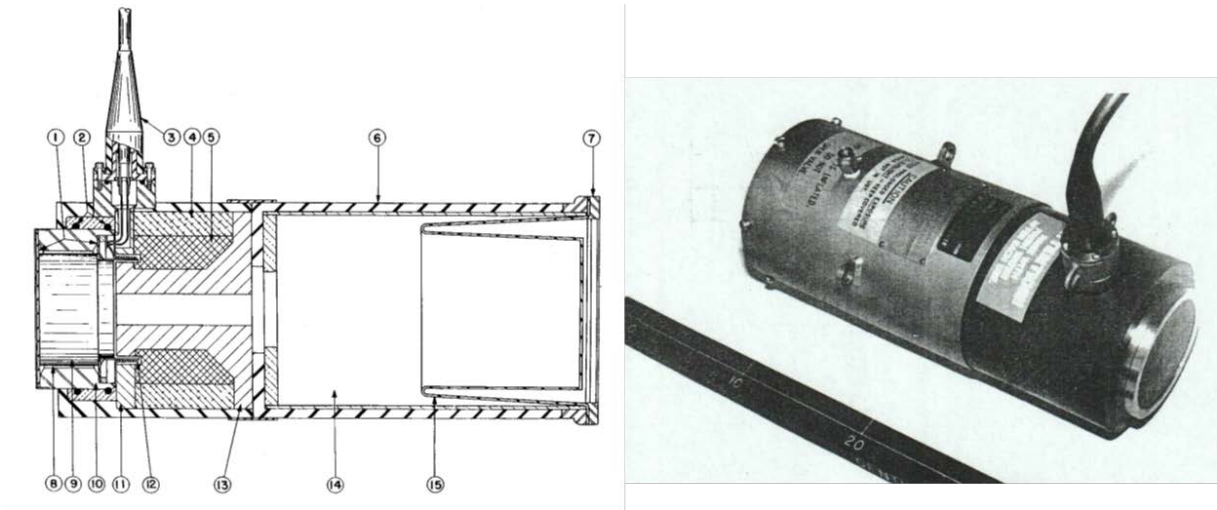


**Figure 12. USRD J9 Moving Coil Projector<sup>25</sup>**

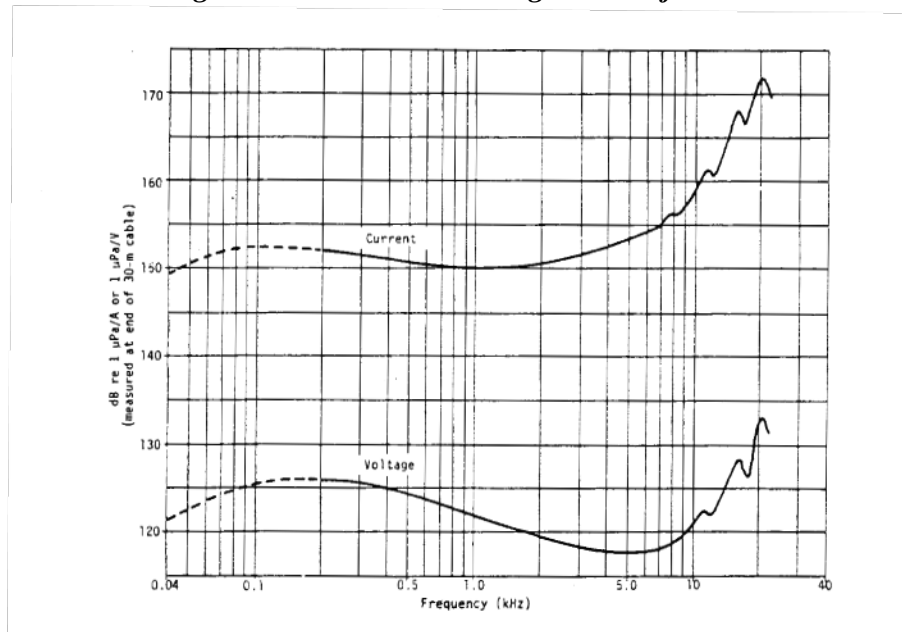


**Figure 13. Typical TVR and TCR for USRD Type J9 Transducer<sup>25</sup>  
(Response below 0.2 kHz is a function of depth.)**

The free-flooded ring (FFR) transducer is a deep depth broadband projector.<sup>26 and 27</sup> The FFR is made from a solid ceramic ring (cylinder) or from multiple wedges shaped ceramic plates bonded together to form larger rings (segmented ceramic ring) as shown in figure 14a. The ceramic ring is protected from the water environment either with a polyurethane or an oil-filled rubber boot FFR. The photograph shown in figure 14b is an example of an oil-filled rubber boot FFR.<sup>28</sup> The FFR produces a double-resonant transmitting pressure response, where the lower-resonance is generated by the inner-cavity of the cylinder acting as a Helmholtz resonator, and the upper resonance is generated by the fundamental circumferential ring resonance that radiates acoustic energy from both the inner and outer surfaces of the cylinder walls. An example of a measured TVR of a FFR is shown in figure 15.<sup>29</sup> This cavity resonance is combined with the “ring” resonance to produce a broad bandwidth transmitting response that is

depth independent. High-power free-flooded rings as big as 4-feet in diameter producing very high source levels below 1-kHz have been used and rings as small as 1-to-4 inches have been used for attaining frequencies above 10-kHz.<sup>26 and 27</sup> To achieve even lower-frequency of operation a free-flooded ring transducer is inserted between two large rigid pipes and is commonly known as a resonant pipe projector.<sup>30, 31, and 32</sup>

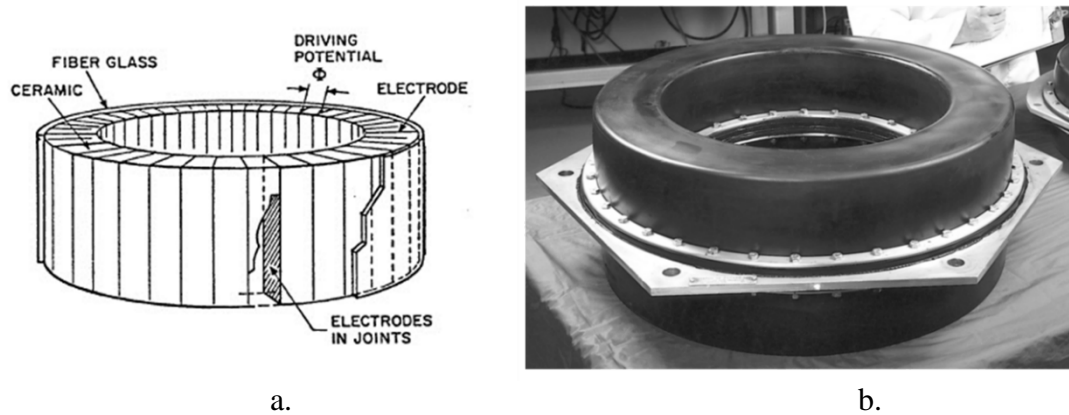


**Figure 14. Free Flooded Ring Transducer**  
(a. ceramic segmented ring and b. photo of oil-filled rubber booted ring.)<sup>28</sup>

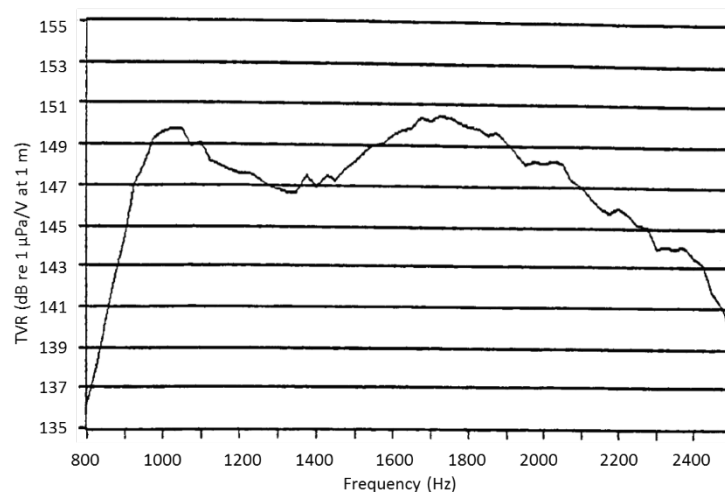


**Figure 15. Example of Measured TVR of a FFR<sup>29</sup>**

Flextensional transducers are a group of transducers that use lever and bending motion to amplify displacement.<sup>33</sup> The most common is the Class IV flextensional transducer as shown in figure 16. The flextensional transducer is composed of an elliptical shaped shell and a ceramic drive stack inserted along its major axis as shown in figure 16a. As the ceramic stack contracts (inward) under ac drive conditions the shell flexes outward at a much greater motion (3-to-4 times) than that of the ceramic stack; and as the ceramic stack expands the shell flexes inward. The shells are of aluminum, steel or fiberglass and the shell/ceramic stack are protected from the water environment with rubber boot and end caps as shown in the photo of figure 16b.<sup>34</sup> These

transducers are typically small compared to wavelength producing nearly omnidirectional beam patterns, have a high-electroacoustic efficiency and produce high source levels and are ideal for low frequency operations. A typical transmitting response is shown in figure 17 untuned and tuned.<sup>35</sup> Large designs that operate at 500-Hz to small designs that operate at 5-kHz have been used.<sup>33</sup> Other flextensional transducer types are the barrel stave transducer (reference 27) and ringshell transducer (reference 36). In addition to flextensional transducers are flexural transducers. These are flexural disc transducers (reference 37), bender bar transducers (reference 15), and slotted cylinder transducers (reference 38).

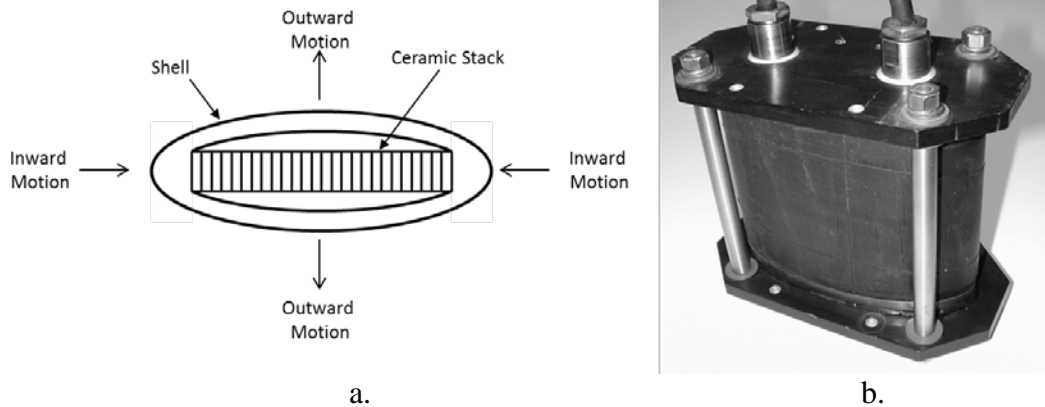


**Figure 16. Flextensional Transducer and Photograph<sup>34</sup>**

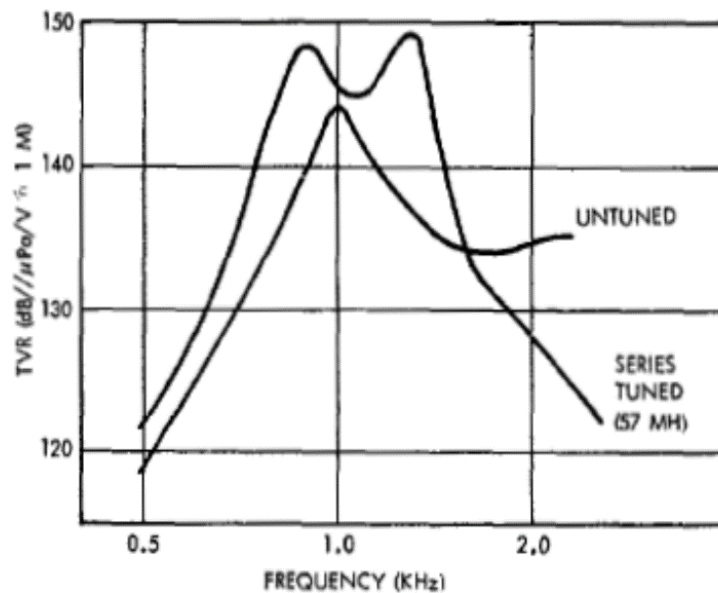
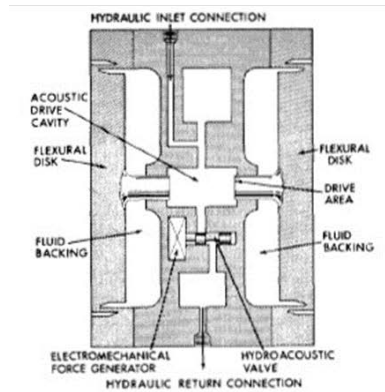


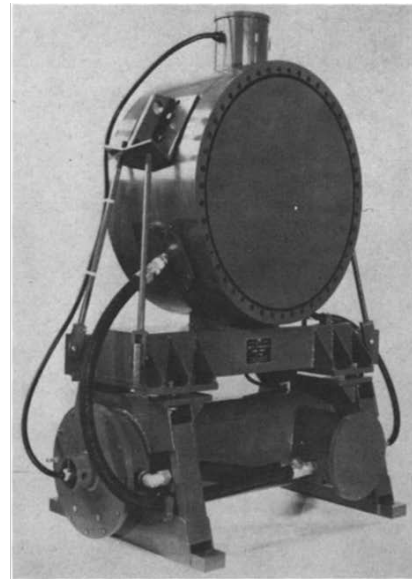
**Figure 17. TVR of Flextensional Transducer<sup>35</sup>  
(Untuned and series tuned.)**

Hydroacoustic projectors have been of interest to the Navy because they can produce high-acoustic output at very low-frequencies. Figure 18a shows a generic hydroacoustic projector operational diagram. The hydroacoustic projector uses hydraulic oil to flow from a pump to the

drive cavity that is modulated by a sliding control valve. The flow modulation varies the pressure in the drive cavity. The drive cavity is connected to radiating diaphragms by drive pistons. The varying pressure in the drive cavity produces a force on the drive pistons that, in turn, forces the diaphragms to vibrate. A two-piston type hydroacoustic source built by General Dynamics is pictured in figure 18b. These devices are big and heavy weighing more than a 1,000 lbs. and typically operate below 50-Hz.<sup>15 and 39</sup> A typical TVR for a hydroacoustic projector is shown in figure 19.<sup>40</sup>



a.



b.

**Figure 18. Hydroacoustic Transducer and Photograph<sup>15</sup>**

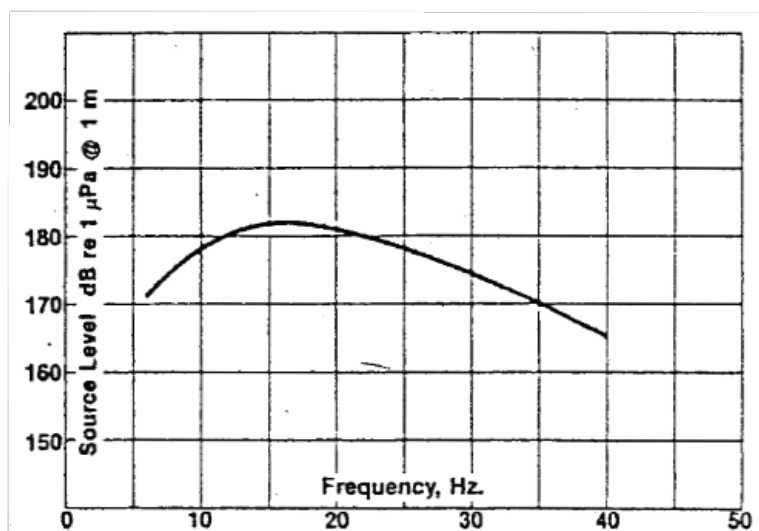


**Figure 19. Typical Transmitting Response for Hydroacoustic Transducer<sup>40</sup>**

Air gun transducers are devices often used in seismic exploration as an energetic source of LF impulsive sound. Air guns are inexpensive sources of high-energy sound impulses in this frequency range below 20-Hz-to-above 100-Hz. All air guns function in the same general way, a container of high-pressure air is momentarily vented to the surrounding water, producing an air-filled cavity. This cavity expands and contracts violently several times. The first few oscillations radiate sound having a waveform that approximates a damped cosine. The fundamental frequency of the waveform depends both upon the maximum radius of the cavity and upon the ambient pressure of the surrounding water. The acoustical energy radiated depends primarily on the initial pneumatic energy in the container and the ambient pressure of the surrounding water. Figure 20a shows an air gun type that blows spherical cavities.<sup>41</sup> In this design, the air storage chamber is sealed with a lid attached to a shuttle that extends upward into a shuttle recoil chamber. When an electrical solenoid is actuated, the shuttle is rapidly blown upward by the stored compressed air. The recoil chamber causes the shuttle to be returned rapidly, resealing the storage chamber. During the interval when the storage chamber is not sealed, the stored air expands through the circumferential air ports and blows an essentially spherical cavity in the surrounding water. Also pictured in figure 20b is a Teledyne Bolt, Model 1900LLX-T Air Gun.<sup>42</sup> Figure 21 gives typical source levels for three types of air guns.<sup>41</sup>

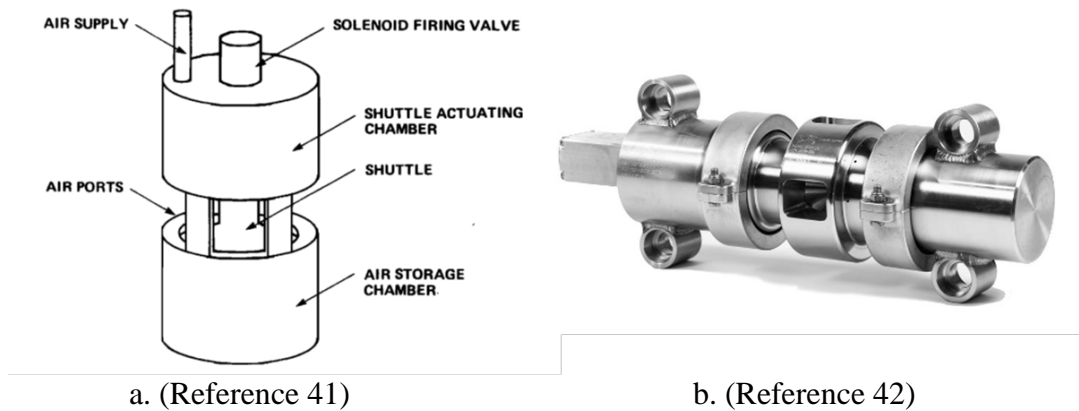


***Figure 20. Air Gun Impulsive Underwater Transducer and Photograph***



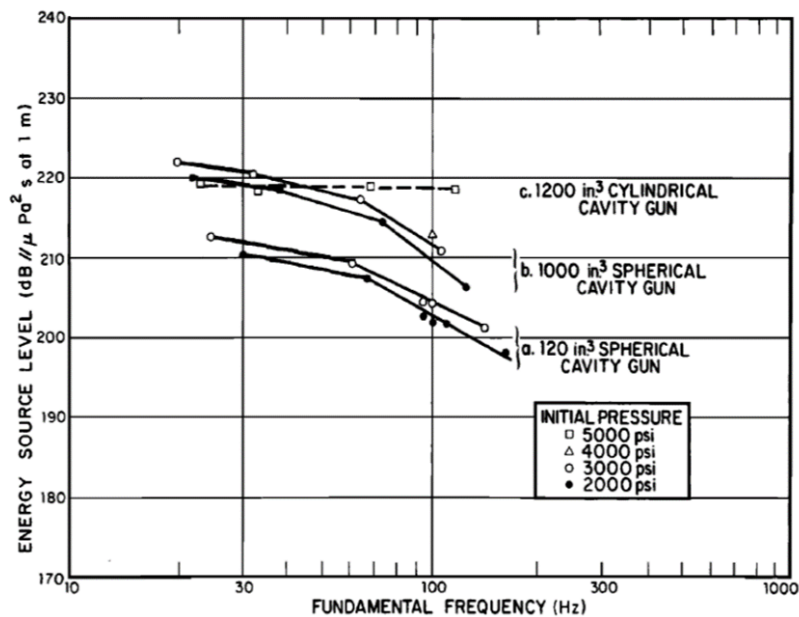


**Figure 21. Energy Source Level Response as a Function of Fundamental Frequency for Three Different Air Guns**  
 (a. Spherical-cavity gun with 120-in.<sup>3</sup> camber.  
 b. Spherical-cavity gun with 1000-in.<sup>3</sup> camber.  
 c. Cylindrical-cavity gun with 1200-in.<sup>3</sup> camber.)<sup>41</sup>

Explosive sources were among the earliest used at sea for seismic exploration. Explosive devices specifically designed to generate underwater sound are called explosive sound sources and typically contain a chemical compound Trinitrotoluene (TNT). Explosive sources can provide the high power and LFs needed to study the structure of the seafloor and to explore for oil and gas. The signals generated by explosions are capable of propagating over hundreds or even thousands of kilometers. The most commonly used underwater explosive sound sources still in use are the a Signal, Underwater Sound (SUS) Mk 64 pictured in figure 22 (reference 43) and the Mk 61 explosive source. The Mk 64 generates a 0.031-kg (0.07-lb) explosive charge and the Mk 61 generates 0.82-kg (1.8-lb) explosive charge.<sup>44, 45, and 46</sup> Figure 23 shows the pressure time waveform from the explosion of a 0.82-kg SUS charge at 102 m depth and the source level measurements in 1/3 octave bands for 0.82-kg SUS charge at 23.5 m, 99.6 m and 194.4 m depth.<sup>45</sup>

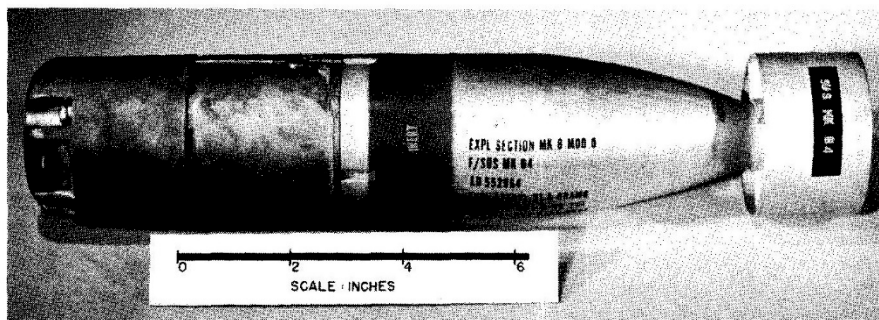


**Figure 22. A Standard U.S. Navy Explosive Sound Signal<sup>43</sup>**

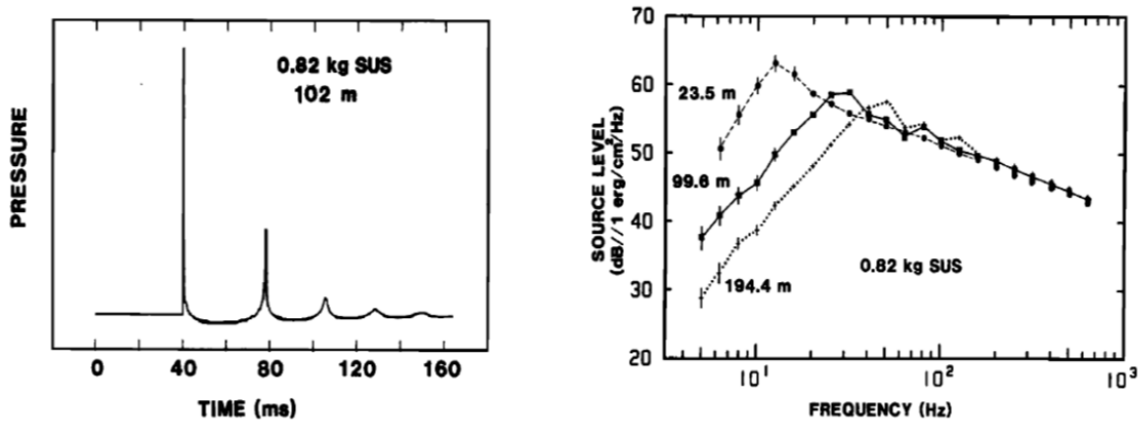


**Figure 23. Pressure Time Waveform from the Explosion of a 0.82-kg SUS Charge at 102 m and Source Level Measurements in 1/3 Octave Bands for 0.82-kg SUS Charges at 23.5 m, 99.6 m and 194.4 m<sup>45</sup>**

## 2.2 THE HYDROPHONE

A hydrophone is a transducer that receives or detects acoustical sound waves. Some are used as oceanographic environmental listening devices, others are used within a sonar system for detection, range and classification purposes, and yet others are used as measurement devices for calibrating a particular sound source or other hydrophones. The majority of sonar receive hydrophones are omnidirectional, at least when measured in the absence of neighboring structures. Omnidirectional hydrophones can be used for passive or active sonar signal reception, and they are typically used below their resonant frequency. Most are small compared to the wavelength of the acoustic signals of interest. The most common types of hydrophones are designed from piezoelectric plates, disc, cylinders, and sphere, which are encapsulated within a polyurethane or rubber jacket. The hydrophone may contain a preamplifier that is part of its encapsulation assembly (wet end) or top side within the ship or boat (dry end).

As discussed earlier, the AN/SQS-23 transducer is both a transmitter and receiver of acoustic pressure. The transmit equivalent circuit in figure 8 can be reconfigured as a receiver equivalent circuit as shown in figure 24 where the input applied voltage  $E_{in}$  source is now an open circuit output voltage  $V_{out}$ . The source driving the circuit is now a force  $F_p$  which is an acoustic pressure  $p$  impinging upon the head mass with surface area  $A_p$ , times a diffraction constant  $D$ , or  $F_p = D A_p p$ , where  $D$  is 2 for a baffled piston. Therefore, the open circuit output voltage  $V_{out}$  is now proportional to the impinging acoustic input pressure. This ratio is known as receiving voltage sensitivity of a transducer (or hydrophone) which relates voltage generated across its terminals to the acoustic pressure of the sound field induced and is denoted as  $M_o = V_{out}/p_{in}$ , where the symbol  $M_o$ , used in general acoustics, stands for “Microphone”. It is customary to express the receiving response as the open-circuit response obtained when the hydrophone works into an infinite preamplifier impedance.

The receiving response is stated as the number of decibels relative to 1-volt produced by an acoustic pressure of one micropascal ( $10^{-6}$  N/m<sup>2</sup>), and written as decibels re 1 V/ $\mu$ Pa and is expressed as,  $RVS(\text{dB re } 1\text{V}/\mu\text{Pa}) = 20 \log M_o = 20 \log V_{out}/p_{in}$ .

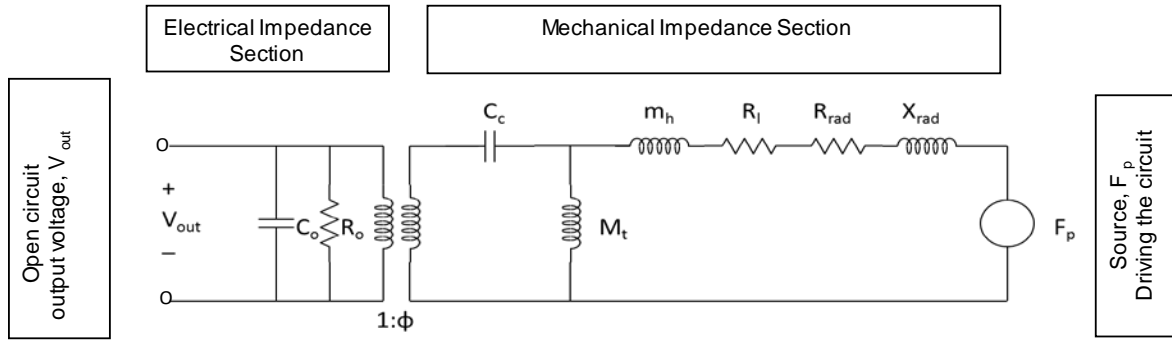


**Figure 24. Transducer Receiving Equivalent Circuit Model**

As an example, for the AN/SQS-23 transducer, an acoustic pressure of  $1\text{-}\mu\text{Pa}$  on the piston surface produces a force  $F_p$  of  $3.08 \times 10^{-8} \text{ N}$  and will generate a voltage of  $1.58 \times 10^{-8} \text{ volts}$  at the terminals or  $-156\text{-dB } 1\text{V}/\mu\text{Pa}$  at  $5\text{-kHz}$  for these circuit values. Thus, a response stated as  $-156\text{-dB re } 1 \text{ volt}/\mu\text{Pa}$  means that the hydrophone generates an open-circuit root-mean-square (rms) voltage of  $1.58 \times 10^{-8} \text{ volts}$  when placed in a plane-wave sound field having an rms pressure of 1 micropascal ( $-120 \text{ dB re pascals}$ ). This is plotted in figure 25 as a function of frequency is the receiving voltage sensitivity response (RVS) for the AN/SQS-23 transducer element. The peak level in the RVS is at the anti-resonance,  $f_a$ , where the impedance is a maximum. For this example, a  $180\text{-dB re } 1\text{-}\mu\text{Pa}$  sound pressure level in water detected by this transducer would develop  $15.8\text{-volts}$  from its terminals as given by  $V_{out} = M_o p_{in}$ .

Typical hydrophone transducers have a receiving voltage sensitivity level of  $-200 \text{ dB}$  to  $-180 \text{ dB re } 1\text{V}/\mu\text{Pa}$ . In this case  $1\text{-volt rms}$  would be developed across its terminals for  $180\text{-dB re } 1\text{-}\mu\text{Pa}$  sound pressure level for a hydrophone that has sensitivity of  $-180 \text{ dB re } 1\text{V}/\mu\text{Pa}$ . The example discussed is an over simplification of a transducers design. Here it did not include the epoxy joint used to bond the ceramic stack together, nor did it include the stress rod and used only one-dimensional circuit analysis techniques. More elaborate circuits that include each piece part would predict more accurate results; plane wave transmission lines that include loss and high-order modes would increase accuracy even more; and a full finite element analysis (FEA) would even be best to produce closer to real world results.

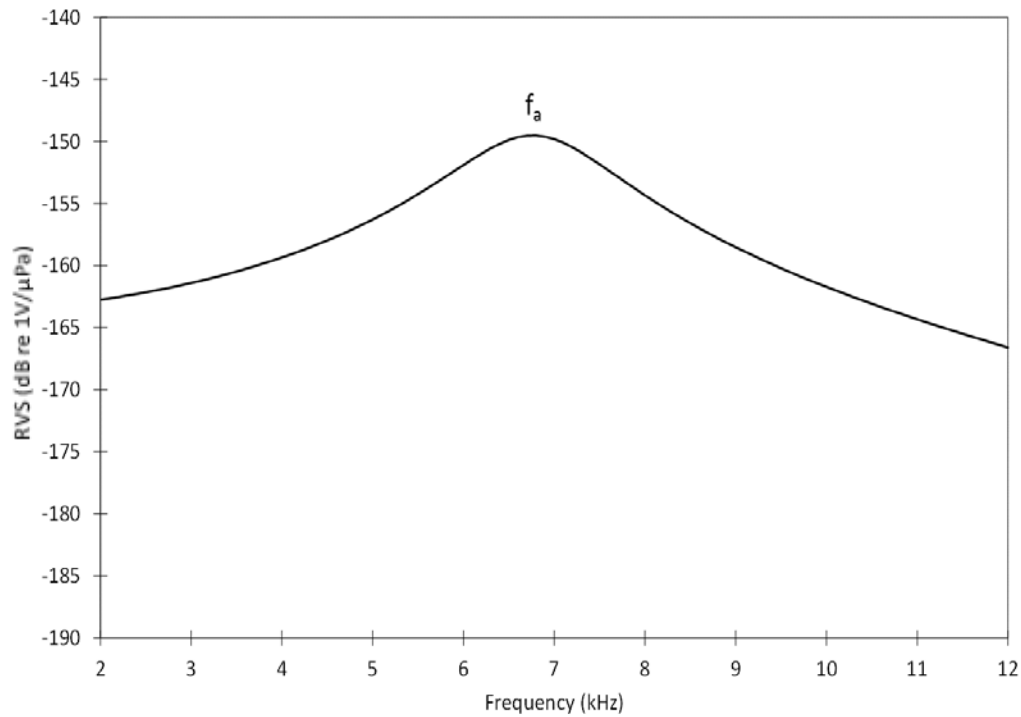


***Figure 25. Transducer Receiving Voltage Sensitivity Response***

A more typical hydrophone shown in figure 26 is the end-capped ceramic cylinder. This type of hydrophone has two piezoelectric cylinders radially polarized through their wall thickness with both the inner and outer surfaces covered with silver electrodes. The piezoelectric cylinders are epoxied together in mechanical series with rigid endcaps epoxied to the ends of the cylinders. The endcaps are typically made of non-active engineered ceramic material such as alumina. The figure shows that the inner surfaces are wired in parallel and the outer surfaces are wired in parallel and connected to a two-conductor underwater cable. The whole cylindrical assembly is encapsulated in a neoprene or polyurethane boot for waterproofing. This type of hydrophone is used well below its resonance where the receiving response is flat and there are no resonant phase shifts.

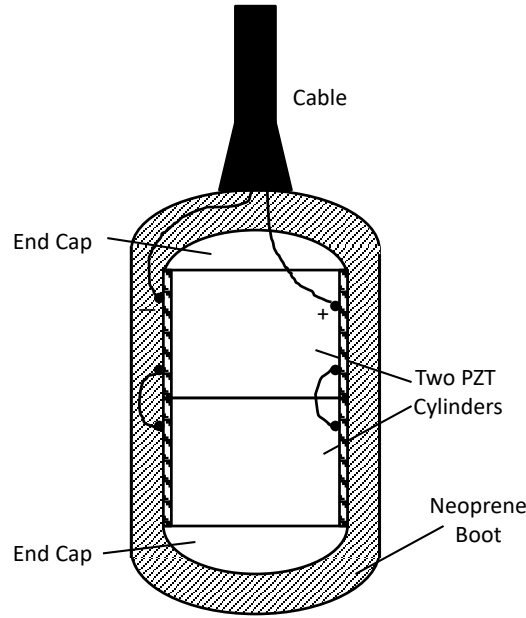


**Figure 26. Capped Cylinder Hydrophone**

The equivalent circuit would be the same as that shown in figure 24 without  $M_t$ , but since one is operating well below resonance one can ignore the masses and radiation impedance. The equivalent circuit can be simplified even further in terms of reflecting the mechanical components (i.e., compliance) of the cylinder over to the electrical side of the circuit. In this case the force  $F_p$  would be divided by the electromechanical transducer turns ratio  $E_p = F_p / \emptyset$  which now has the units of volts and the compliance  $C_c$  multiplied by the square of the electromechanical transducer turns ratio  $C_x = \emptyset^2 C_c$ , which now has the units of Farads. The all-electric equivalent circuit of a hydrophone is shown in figure 27, and since dielectric loss is low  $R_o$  is not needed here. Thus, the sensitivity is a result of the compliance and capacitance of the ceramic cylinder. The open circuit output voltage  $V_{out}$  is now obtained from the transformed force  $E_p$  and a voltage divider of the compliance and capacitance as  $V_{out} = (C_x / (C_x + C_o)) E_p$ . For a radially polarized ceramic cylinder the turn ratio is given by  $\emptyset = (d_{31} / s_{11}^E) 2\pi h$ ; clamped capacitance is  $C_o = C_f (1 - k_{31}^2)$ ; free capacitance is  $C_f = A_c K^T \epsilon_o / w$ ; ceramic compliance is given by  $C_c = s_{11}^E a_m / (2\pi w h)$ , and force as stated earlier is  $F_p = D A_c p$ . Here,  $h$  is the height of the piezoelectric cylinder,  $w$  is the wall thickness of a piezoelectric cylinder, and  $D$  is the diffraction constant ( $D=1$  at frequencies well below resonance for an omnidirectional receiver). The quantity  $d_{31}$  is the piezoelectric strain constant ( $171 \times 10^{-12} \text{ m/V}$  for PZT-5A),  $s_{11}^E$  is the short-circuit piezoelectric elastic constant ( $16.4 \times 10^{-12} \text{ m}^2/\text{N}$  for PZT-5A),  $k_{31}$  is the piezoelectric coupling coefficient ( $0.34$  for PZT-5A),  $K^T$  is the free piezoelectric dielectric constant ( $1700$  for PZT-5A), and  $\epsilon_o$  is permittivity of free space. The quantity,  $A_c$  is the surface area of the piezoelectric cylinder  $\pi D_m h$ , where  $D_m$  is the mean diameter of the piezoelectric cylinder.

For a radially polarized ceramic cylinder with an outside diameter (OD) of 50.8-mm, inside diameter (ID) of 45.7-mm, and a height of 25.4-mm; the calculated equivalent circuit values for  $\emptyset$  is 1.66,  $C_f$  is 22.8 nF,  $C_o$  is 20.2 nF,  $C_c$  is  $9.76 \times 10^{-10} \text{ m/N}$ , and  $F_p$  is  $3.85 \times 10^{-9} \text{ N}$  when  $p$  is 1  $\mu\text{Pa}$ . Therefore,  $C_x$  is 2.7 nF and  $E_p$  is  $2.31 \times 10^{-9}$  volts. The resonance of the cylinder can be calculated by  $f_r = 1 / (\pi D_m) \sqrt{(1 / (s_{11}^E \rho))}$  and anti-resonance can be calculated by  $f_a =$

$f_r/\sqrt{1 - k_{31}^2}$ , where  $\rho$  is the density of the PZT-5A material (7,700 kg/m<sup>3</sup>). For this cylinder the resonance frequency is 18.6 kHz and the anti-resonance frequency is 19.8 kHz. The calculated receive voltage sensitivity ( $V_{out}$ ) of the radially polarized ceramic cylinder is  $2.73 \times 10^{-10}$  V/ $\mu$ Pa from the values  $C_o$ ,  $C_x$  and  $E_p$ . For  $V_{out}$ , in decibels the RVS is -191.3 dB re 1V/ $\mu$ Pa. The equivalent circuit of a hydrophone of figure 27 can be further reduced to that of figure 28, where the source is now an equivalent thevenin source  $V_{out}$  in series with the free capacitance  $C_f$  given by  $C_o + C_x$ . The RVS can also be simply calculated from  $M_o = g_{31}a_m$  for an end capped ceramic cylinder where  $g_{31}$ , the piezoelectric stress constant, is ( $11.4 \times 10^{-12}$  V•m/N for PZT-5A) and mean radius  $a_m$  is 24.1-mm. Thus,  $M_o$  is  $2.75 \times 10^{-4}$  V/Pa or  $2.75 \times 10^{-10}$  V/ $\mu$ Pa and RVS is -191.2 dB re 1V/ $\mu$ Pa. For two cylinders wired in parallel the sensitivity would stay the same but the capacitance would double.

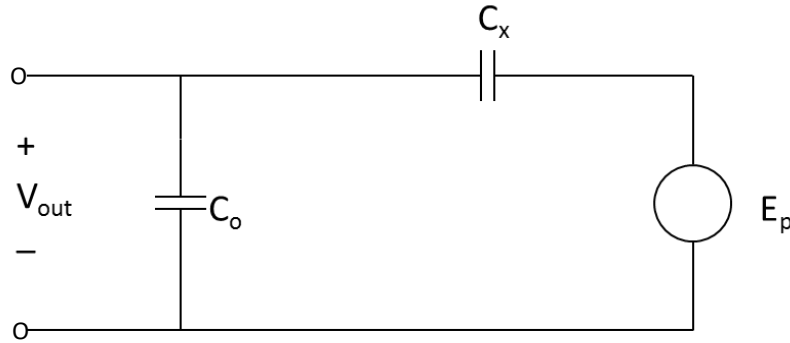


**Figure 27. Equivalent Circuit of a Hydrophone**

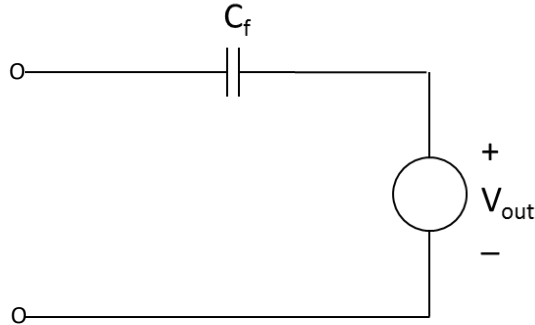


**Figure 28. Circuit of a Hydrophone Further Reduced**

Another common type of hydrophone is the spherical hydrophone such as the NUWC USRD Type F42C transducer as shown in figure 29. This is a standard hydrophone that can be rented as part of the U.S. Navy NUWC USRD standard loan transducer program. Each hydrophone is issued with an individual calibration curve free-field voltage sensitivity (FFVS) or receive voltage sensitivity (RVS) curve at the end of an electrical cable. This hydrophone is a reversible transducer and may be used also as sound source as well as a receiver.<sup>47</sup>

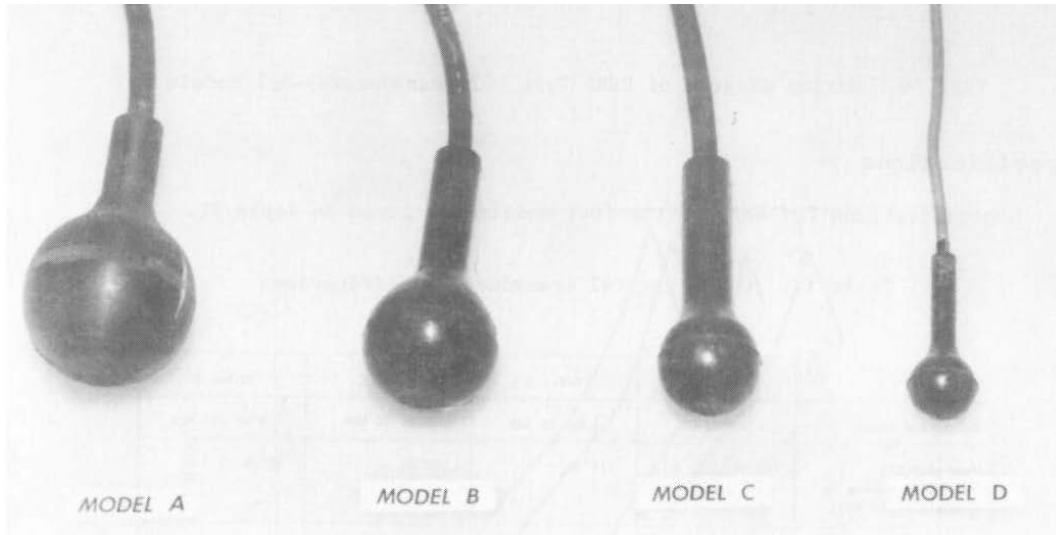


**Figure 29. The F42 Transducers<sup>47</sup>**

The active elements are two PZT-4 hemispheres bonded together, wired with a two-lead connector cable and encapsulated in polyurethane. The F42C PZT sphere dimensions are OD is 2.54-cm and wall thickness is 3.2-mm, ID is 1.9-cm, and the mean diameter ( $D_m$ ) is 2.22-cm. The sensitivity of the ceramic sphere is also a result of the compliance and capacitance as in the ceramic cylinder. The open circuit output voltage  $V_{out}$  is obtained as was given in the ceramic cylinder example. For a radially polarized ceramic sphere the turns ratio is given by  $\phi = (d_{31}/s_c^E)4\pi a_m$ ; clamped capacitance is  $C_o = C_f(1 - k_p^2)$ ; free capacitance is  $C_f = A_c K^T \epsilon_o/w$ ; ceramic compliance is given by  $C_c = s_c^E/(4\pi w)$ ; and force is  $F_p = DA_c p$ . The quantity,  $w$  is the wall thickness of a piezoelectric sphere,  $D$  is the diffraction constant ( $D=1$  at frequencies well below resonance for omnidirectional receiver),  $d_{31}$  is the piezoelectric strain constant ( $122 \times 10^{-12}$  m/V for PZT-4),  $s_c^E$  is the short-circuit piezoelectric elastic constant  $(s_{11}^E + s_{12}^E)/2$ , where  $s_{11}^E = 12.3 \times 10^{-12}$  m<sup>2</sup>/N and  $s_{12}^E = -4.2 \times 10^{-12}$  m<sup>2</sup>/N for PZT-4,  $k_p$  is the planar piezoelectric coupling coefficient (0.58 for PZT-4),  $K^T$  is the free piezoelectric dielectric constant (1300 for PZT-4),  $\epsilon_o$  is permittivity of free space, and  $A_c$  is the surface area of the piezoelectric sphere  $4\pi a_m^2$ , where  $a_m$  is the mean radius of the piezoelectric sphere.

For this radially polarized ceramic sphere the calculated equivalent circuit values are as follows:  $\phi$  is 4.2,  $C_f$  is 5.5 nfd,  $C_o$  is 3.7 nfd,  $C_c$  is  $101.5 \times 10^{-12}$  m/N, and  $F_p$  is  $1.55 \times 10^{-9}$  N when  $p$  is 1- $\mu$ Pa. Therefore,  $C_x$  is 1.8 nF and  $E_p$  is  $3.7 \times 10^{-10}$  volts. The resonance of the sphere can be calculated in the same manner as for the cylinder but with  $s_c^E$  being substituted for  $s_{11}^E$ .  $\rho$  is the density of the PZT-4 material ( $7600$  kg/m<sup>3</sup>) for this sphere. The resonances frequency is 81.6 kHz and anti-resonance frequency  $f_a$  is determined from  $f_a = f_r/\sqrt{1 - k_p^2}$  equals 100.2-kHz. The receive voltage sensitivity ( $V_{out}$ ) of the radially polarized ceramic sphere is  $1.2 \times 10^{-10}$  V/ $\mu$ Pa for the values  $C_o$ ,  $C_x$  and  $E_p$  and in decibels the RVS is -198.4 dB re 1V/ $\mu$ Pa. With a 30-meter test cable the RVS is reduced to -206 dB re 1V/ $\mu$ Pa because of the additional added cable capacitance of 8 nF added to  $C_o$ . Figure 30 shows typical FFVS responses of the F42 transducers for different PZT element sphere sizes. F42A is 5-cm in diameter, F42B is 3.81-cm, F42C is 2.54-cm, and F42D is 1.27 cm. The dip in the responses right before the resonant peak

is a result of diffraction caused by the element starting to become large compared to acoustic wavelength, where in this case  $D$  is no longer 1.

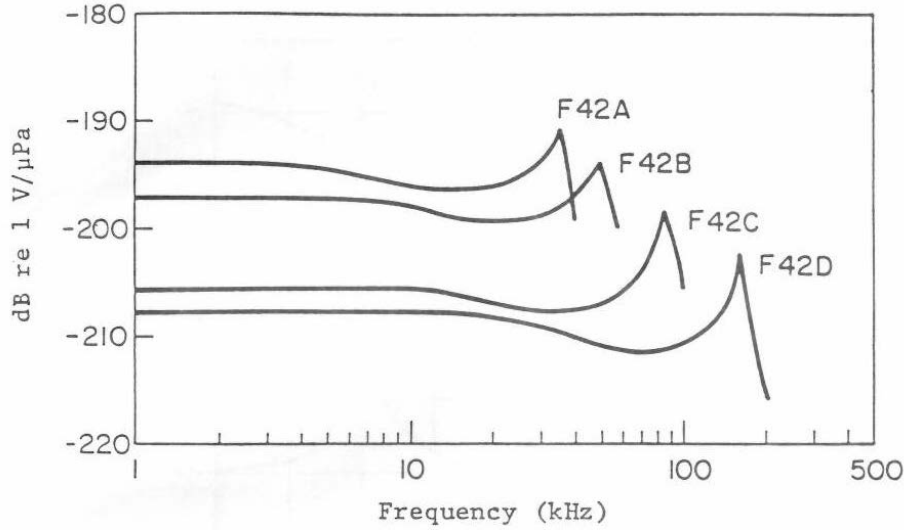


**Figure 30. Typical FFVS for the F42 Transducers<sup>47</sup>**

### 2.3 HYDROPHONE PREAMPLIFIERS AND SELF NOISE

Hydrophone preamplifiers are low-power amplifiers for receiving. They have high-input impedances with adjustable or unity gains. The hydrophone may contain a preamplifier that is part of its encapsulation assembly (wet end) or topside within the ship or boat (dry end). The input impedance of the preamplifier is high enough that it will not reduce the sensitivity of the hydrophone and its output impedance is low enough that the receive signal (now a voltage) would not be reduced with any additional cabling added. Gain is added to the preamplifier to increase a weak signal for electronic processing and to increase the signal above the noise source levels going forward.

Noise sources can strongly influence the hydrophones capability to detect weak low-level manmade signals from that of environmental or self-noise signals. The noise sources are sea environmental noise, ambient acoustic noise, hydrophone self-noise and amplifier self-noise. The sea environmental noise and ambient acoustic noise levels are discussed in further detail in reference 43. The hydrophone self-noise is the electrical noise in the stiffness-controlled regime (below resonance) due to thermal agitation caused by electrical and mechanical losses of the hydrophone. The thermal agitation can be represented by Johnson thermal noise voltage given by  $E_n^2 = 4KT\Delta fR$ , where  $K$  is the Boltzmann's constant ( $1.381 \times 10^{-23}$  J/K),  $T$  is the absolute temperature ( $290^\circ\text{K}$ ),  $\Delta f$  is the frequency bandwidth (Hz) and  $R$  is the radiation and loss resistances.

At low-frequencies the loss mechanism resistance is controlled by the equivalent series resistance  $R_s$  of dielectric losses  $R_o$  of the hydrophone. The equivalent series resistance is given by  $(\tan(\delta)/\omega C_f)$ . The hydrophone self-noise can be represented as an additional voltage source in dB as  $20\text{Log}(E_n) = -198 \text{ dB} + 10\text{Log}(R_s) + 10\text{Log}(\Delta f)$  to the equivalent circuit. It is often



desirable to determine the hydrophone self-noise in terms of an equivalent noise pressure so it can be compared directly with that of the ambient ocean noise sources. It is known that the sensitivity of a hydrophone is the open circuit voltage per applied acoustic pressure i.e.,  $M_o = V_{out}/p$ . If  $V_{out}$  is the noise source  $E_n$  then the equivalent noise pressure is  $p_n = E_n/M_o$ . The equivalent noise pressure is then given by  $20\text{Log}(p_n) = -198 \text{ dB} + 10\text{Log}(R_s) + 10 \text{Log}(\Delta f) - RVS$ . Typically, the hydrophone equivalent noise pressure level should be below that of the ambient ocean noise level. This is also true for that of the preamplifier; that is to say, its own self-noise level should be below that of the ambient ocean noise level.

A USRD H56 measurement hydrophone with a low-noise preamplifier and its open circuit FFVS response at the end of a 23-m cable is shown in figures 31 and 32. It operates from 10-Hz-to-65-kHz and has nominal FFVS of  $-171 \text{ dB re } 1\text{V}/\mu\text{Pa}$  with a preamplifier gain of 12 dB (X4). An example of a noise curve for the H56 hydrophone preamplifier is shown in figure 33. At 1-kHz the voltage noise level is  $-155 \text{ dB re } V/\sqrt{\text{Hz}}$  or  $20 \text{ nV}/\sqrt{\text{Hz}}$  with a 100 pF capacitor across the input. This is a typical noise level of some preamplifier designs (some are as low as  $2 \text{ nV}/\sqrt{\text{Hz}}$ ). When comparing the H56 hydrophone noise level to an ambient ocean acoustic pressure noise level for sea state zero at 1-kHz (i.e.,  $44 \text{ dB re } \mu\text{Pa}/\sqrt{\text{Hz}}$ ) the hydrophone noise level ( $25 \text{ dB re } \mu\text{Pa}/\sqrt{\text{Hz}}$ ) is about 19-dB lower in noise level than ambient ocean acoustic pressure noise level as shown in figure 34. This is for hydrophone sensitivity (without preamplifier) of  $-183\text{-dB}$ , capacitance of 100-pF,  $\tan \delta$  of 0.006 or  $R_s$  equal to 10-kohms. The equivalent voltage noise level for the hydrophone is  $-158 \text{ dB } V/\sqrt{\text{Hz}}$ , slightly lower than the preamplifier noise level.<sup>25, 47, 48, 49, and 50</sup>

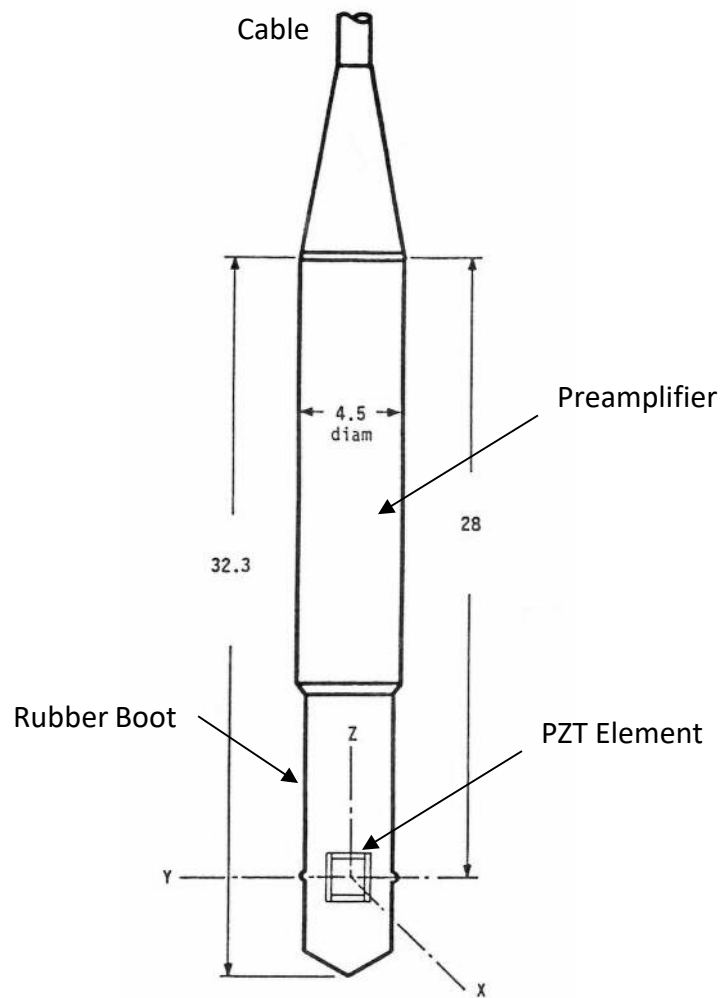


**Figure 31. Measurement Hydrophone, Dimensions in Centimeters<sup>47</sup>**

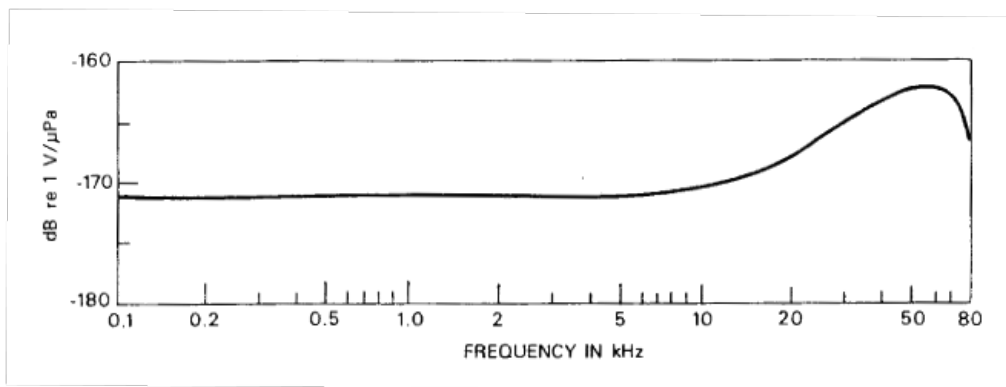


**Figure 32. Typical Open-Circuit FFVS of USRD Type H56 Hydrophone at End of 23-m Cable<sup>47</sup>**

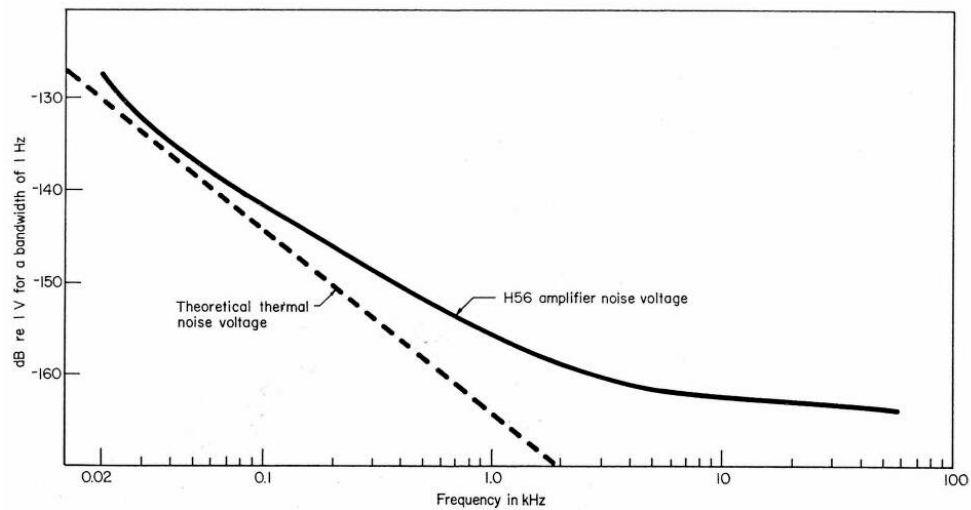


**Figure 33. Noise Voltage at Input of USRD Low-Noise Amplifier for H56 Hydrophone, 100-pF Source<sup>48</sup>**

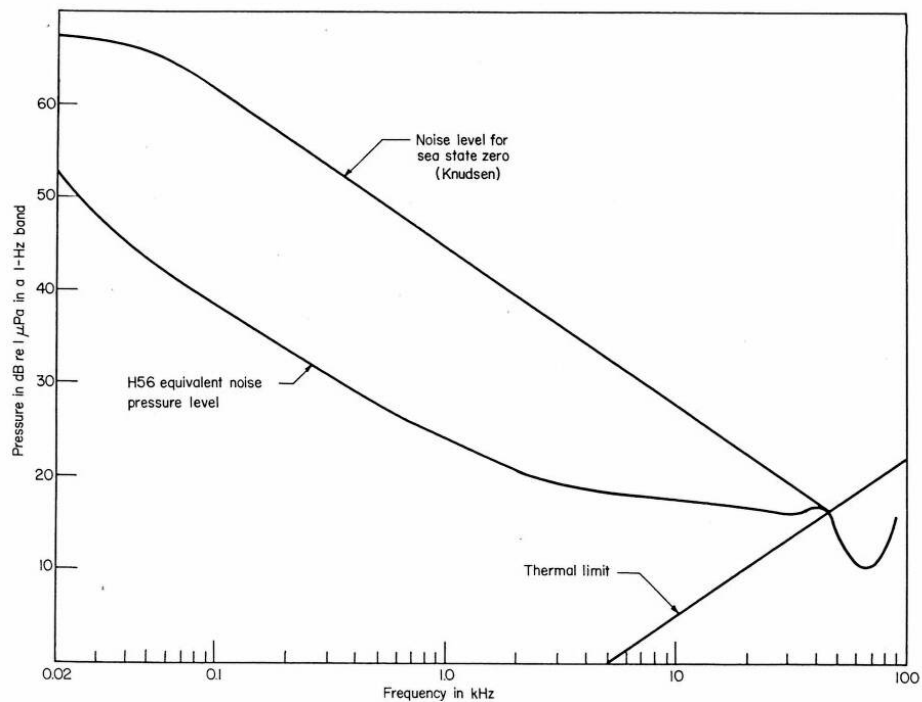


**Figure 34. Equivalent Noise Pressure Level of H56 Hydrophone Compared with the Noise Level of Sea State Zero<sup>48</sup>**

## 2.4 VECTOR HYDROPHONES AND SENSORS

The previous hydrophones discussed are small compared with acoustic wavelength and have an omnidirectional beam pattern within their operating frequency band. Hydrophones or sensors that have a directional beam pattern or unidirectional beam patterns are called vector

hydrophones or sensors. Vector hydrophones or sensors include the Pressure Gradient Hydrophones, Acoustic Motion Sensor, and Multimode sensors which achieve directionality within a small package, as compared to a large array of many hydrophones to achieve directionality. Vector hydrophones or sensors are capable of forming a dipole (figure-eight) type beam pattern or cardioid type beam pattern or super-cardioid (Limacon) beam patterns, as shown in figure 35. A directional beam such as the cardioid has the ability to discriminate or detect a target from either the left or right in the case of towed arrays or sonobuoys, where omnidirectional hydrophones do not.<sup>51</sup>

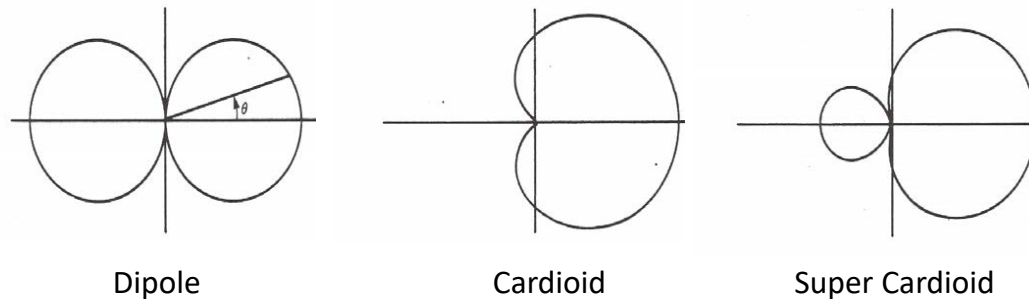


**Figure 35. Vector Sensor Beam Pattern Types<sup>51</sup>**

Pressure Gradient Hydrophones consist of two omnidirectional pressure-sensing elements that are spaced close together and if the hydrophone spacing is small compared to the acoustic wavelength, a directional response results. As the name suggests, this type of hydrophone subtracts the outputs of the two hydrophones, giving a change in pressure per distance increment ( $\Delta p = p_2 - p_1$ ). This change in pressure is related to the particle velocity  $u$  by  $\partial p / \partial r = j\omega\rho u$ . The pressure gradient hydrophones can sense in different directions and thus are a vector quantity in contrast to the omnidirectional pressure hydrophone which is a scalar quantity that senses from all directions. The pressure gradient hydrophones have directional sensitivities in the form of a “figure eight” or cosine dipole type pattern. A dipole pattern can be developed by two (180-degrees) out-of-phase omni sensors separated by less than half-wavelength spacing as shown in figure 36. As the spacing is reduced between elements the dipole pattern level is reduced. Characteristics of a dipole beam pattern are that it has a constant 3-dB down beam width of 90-degrees, nulls at 90- and 270-degrees, and a directivity index (DI) of 4.8-dB. A cardioid pattern can be developed in two ways: in one rendition, two omnidirectional sensors are separated by a quarter wavelength spacing with one of the sensors phase-shifted (delayed) by 90-degrees as shown in figure 37a. In another rendition, three omni sensors are used with two sensors 180-degrees out-of-phase and a third sensor displaced by less than half a wavelength as shown in figure 37b. Both methods are commonly used. The cardioid pattern in figure 37a has a 3-dB down beam width of 180-degrees, a null at 180-degrees, and a DI of 3.0-dB. The cardioid pattern in figure 37b has a 3-dB down beam width of 131-degrees, 6-dB down beam width of 90-degrees, a null at 180-degrees, and a DI of 4.8-dB (the same DI as the dipole). The super-cardioid pattern in figure 35 which is more directive can be produced with one of the sensors in figure 37a phase-shifted (delayed) by 30-degrees. The super-cardioid has a 3-dB down beam width of 115-degrees and is 8.6-dB down at 90-degrees. The back lobe is 11.7-dB down from front main lobe and the DI is 5.7-dB. There is also a hyper-cardioid that has a 3-dB down beam width of 105-degrees, is 12-dB down at 90-degrees, with a back lobe of 6-dB down from the front main lobe and with a DI of 6-dB.

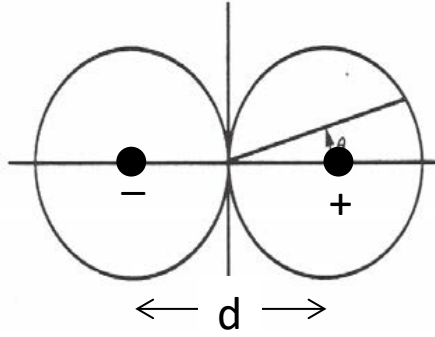


**Figure 36. The Dipole Sensors, Two Out-of-Phase Omni Sensors Spaced  $d \leq \lambda/2$**

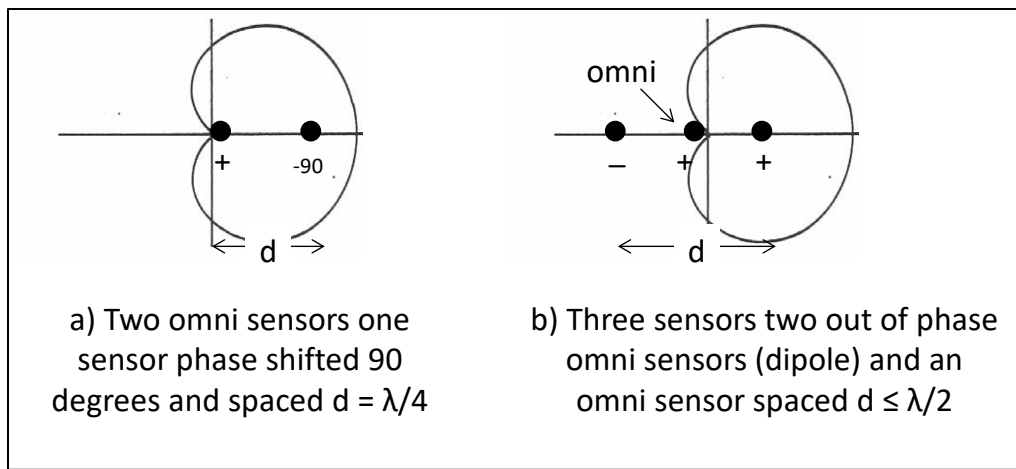


**Figure 37. The Cardioid Sensor**

Vector dipole sensors are often tested or calibrated in a nearfield environment in a tank or pond where the wave front is spherical at low frequencies using a standard reference pressure hydrophone such as a H56 for comparison and a standard sound source such as a J9 projector (1-to-5 meters apart). In calibration the range between the source and receiver is often such that  $r/\lambda$  is not very large, which is in the nearfield. For comparison calibration between two different pressure hydrophones such as a known hydrophone (H56) and unknown hydrophone testing in the nearfield has no effect on the relative levels since the pressure is the same on the two, and since the two are positioned at the same distance from the source. However, for comparison of a vector sensor with a pressure sensor (hydrophone) in the nearfield, its receiving voltage sensitivity level is overestimated caused by spherical spreading and a correction factor is required. If a comparison test is performed in the farfield where the acoustic pressure wave is planar, the measurement is direct and no correction is required, but would require a lake test facility in order to test in the farfield. The correction factor is the ratio of pressure  $p_s$  and particle velocity  $u_s$  of a spherical point source to that of the ratio of plane wave pressure  $p_p$  and particle velocity  $u_p$ . The correction factor magnitude in dB is given as,  $10 \log(1 + \lambda^2/(2\pi r)^2)$ , and phase  $\phi = \tan^{-1}(\lambda/2\pi r)$  which must be subtracted from the measured sensitivity when the

vector sensor is calibrated with a standard pressure hydrophone in the nearfield. Figure 38 shows the relative spherical wave pressure, velocity and correction factor as a function of range and wavelength. It can be seen that for small values of  $r/\lambda$ , the velocity and pressure diverges and the plane wave relationship  $p=\rho cu$  is not valid and the correction can be quite high, i.e., greater than 10 dB at  $r/\lambda=0.05$ . It can also be seen that the correction is less than 0.5-dB when  $r/\lambda=0.5$  and 0-dB when the range and wavelength are equal and a plane wave relationship is valid.<sup>25</sup>

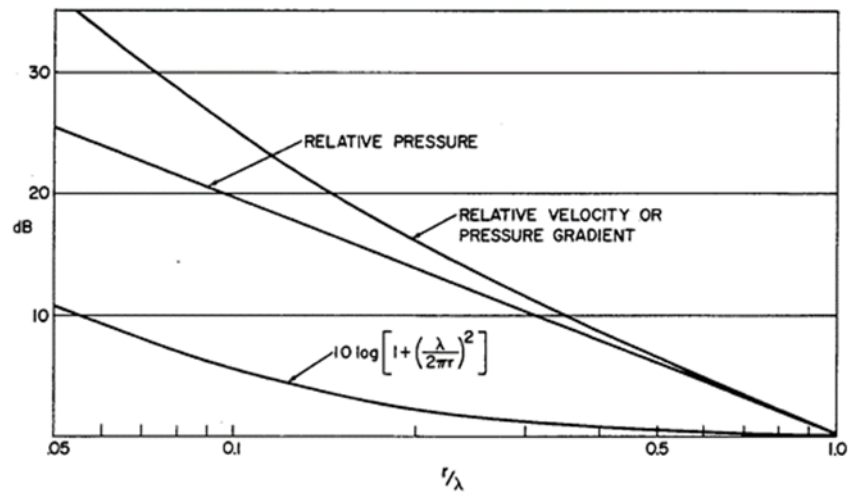
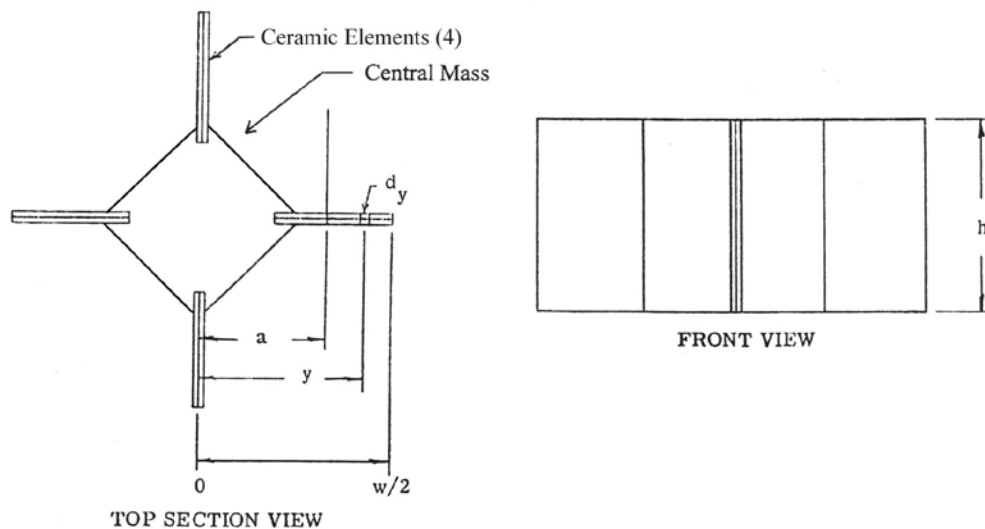


**Figure 38. The Relative Spherical Wave Pressure and Velocity as a Function of Range and Wavelength<sup>27</sup>**

An example of a pressure gradient hydrophone is the directional low-frequency analysis and recording (DIFAR) hydrophone used in some versions of the AN/SSQ-53 Sonobuoy and shown in figure 39. This design forms two directional sine and cosine patterns that are developed by orthogonal ceramic bender ceramic vanes, with the addition of an omnidirectional hydrophone (e.g., ceramic disk) mounted to the central mass a cardioid-type beam patterns could be developed.<sup>52 and 53</sup>



#### Ceramic Vane Directional Hydrophone Layout

Note : Addition of an Omni Hydrophone (e.g. Ceramic Disk) to the Central Mass unit is an example of a DIFAR Hydrophone array used in some versions of the AN/SSQ-53 Sonobuoy

(Reference 53)

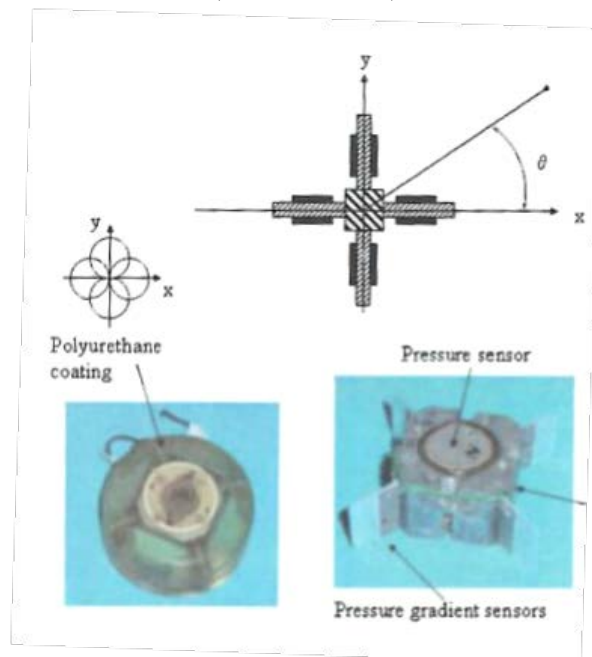


**Figure 39. Ceramic Vane Pressure Gradient Hydrophone<sup>52</sup>**

The Acoustic Motion Sensor responds to the particle motion associated with the acoustic pressure field. The Acoustic Motion Sensor response can be proportional to displacement, velocity, or acceleration. These sensors are built in a variety of ways. A Geophone (used in the seismic industry) is an acoustic motion (velocity) sensor. One type is the inertial hydrophone type shown in figure 40. Typically, they are neutrally buoyant so that the hydrophone will move with the net particle motion of the medium (water). This Geophone is an electrodynamic type

which has a central inertial mass with a coil wrapped around it, a simplified illustration of it operating is shown in figure 40a. The inertial mass is connected to a hydrophone case through a spring that is used for restoring the center of the hydrophone when not in motion. A magnet is connected to hydrophone case, and as the hydrophone case and magnet move up and down with particle motion around the inertial mass and coil, a voltage is induced in the coil that is proportional to the speed of the motion. Figure 40b shows a photograph of a Geospace, Inc. Model GS-14-L9 low-cost commercially moving coil type geophone.<sup>54 and 55</sup>

An example of a two-axes dipole hydrophone with a piezoelectric disc located in the third axis is shown in figure 41. The dipole sensor uses two Geospace, Inc. model GS-14-L9 geophones pictured to the right in figure 41. These geophones are 19.1-mm in diameter, 18.8-mm in length, and have an on-axis velocity sensitivity of 23.6 V/(m/s) or 27.5 dB re V/(m/s) above resonance. Two geophones are orthogonally mounted to one-another and encapsulated in syntactic foam (epoxy with embedded micro-balloons) to make the complete sensor near neutrally buoyant. The measured acoustic sensitivity compared with modeled results is shown in figure 42. The sensor was tested in the nearfield and its pressure sensitivity response level needed to be corrected or a correction factor applied. For a radial test distance of 5.3-m at 60-Hz, the correction factor is 1.7-dB and phase is 35.3-degrees, using a speed of sound of 1,425-m/s. The farfield acoustic pressure sensitivity can be predicted from velocity sensitivity using  $M_o = V_{out}/p_{in} = (1/\rho c)(V/u)$  where  $p_{in} = \rho c u$  for a plane wave. The voltage to velocity ratio  $V/u$  is the velocity sensitivity for the geophone sensor. Therefore, predicted receive sensitivity  $20 \log M_o$  is -96 dB re 1 V/Pa and referenced to a  $1 \mu Pa$  is -216 dB re 1 V/ $\mu Pa$  at 60-Hz, which is close to the corrected measured results shown in figure 42. The measured and modeled receive acoustic directivity beam patterns around one of the geophones axes are shown to the right in figure 42 at 100-Hz, the measured beam pattern is a well formed dipole.<sup>56</sup>

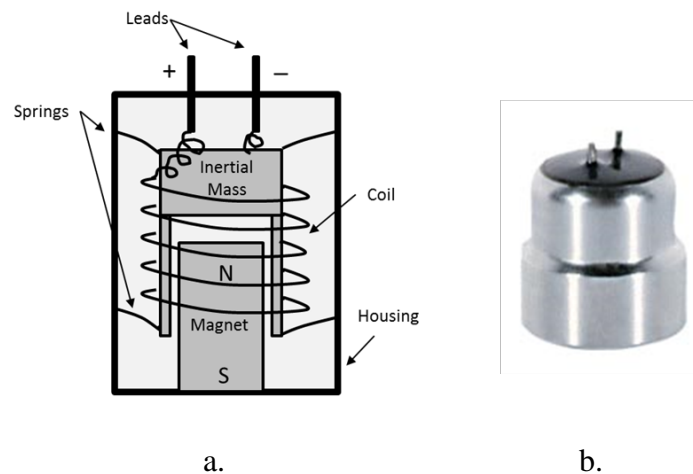


**Figure 40. Geophone Acoustic Motion Sensor<sup>54 and 55</sup>**



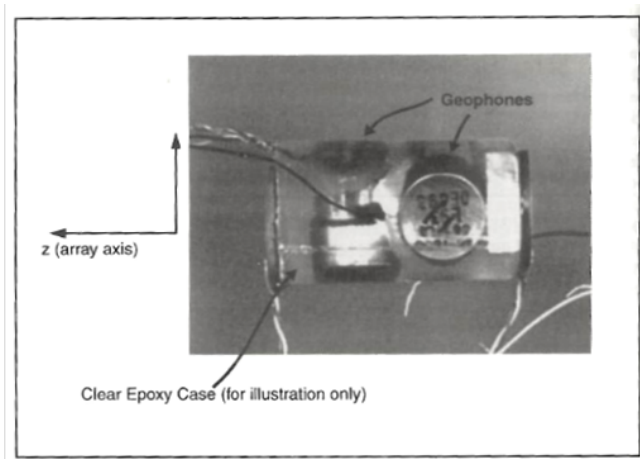
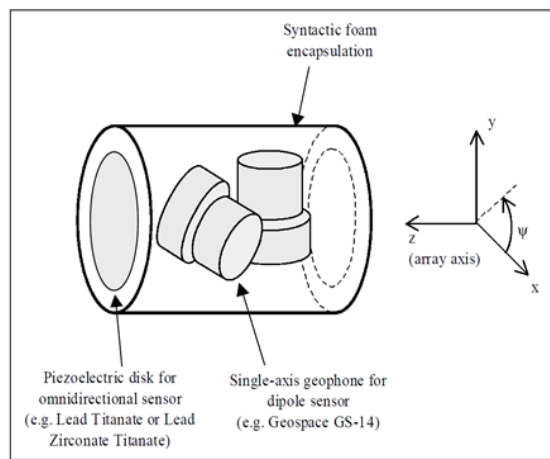


**Figure 41. Two-Axis Dipole Hydrophone<sup>56</sup>**

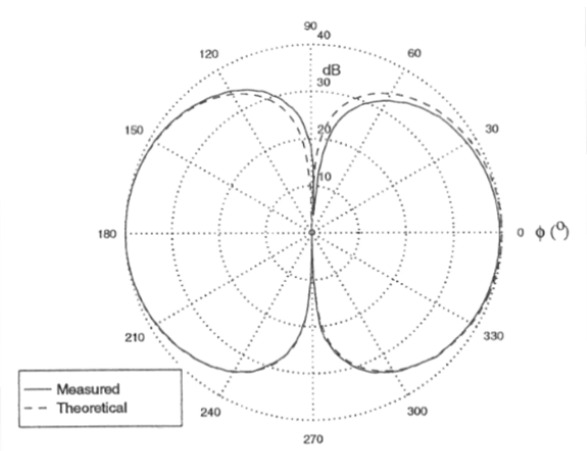
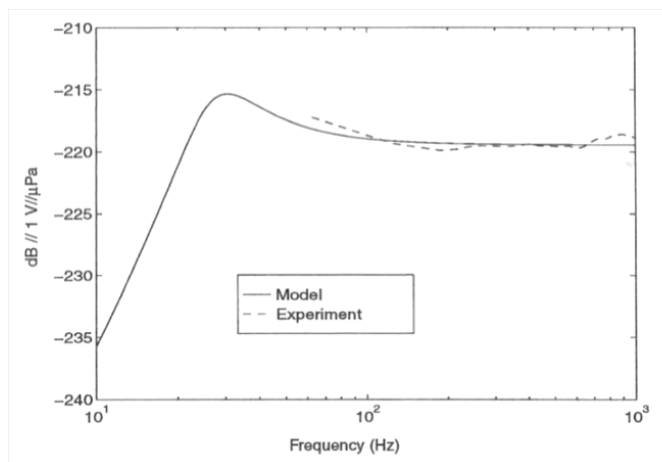


**Figure 42. Measured Acoustic Sensitivity and Beam Pattern of Geophone<sup>56</sup>**

Another example of a single-axis acoustic motion (velocity) sensor is shown in figure 43. This is a neutrally buoyant bimorph flexural disk accelerometer mounted on a pressure release surface baffle. The sensing element is a piezoceramic bimorph disk, wired so as to be sensitive to bending. The edge of the disk is attached to the inside cylindrical pressure tight aluminum housing (shell) which acts as the inertial mass. The syntactic foam around the housing makes the device neutrally buoyant which makes the motion of the sensor same as the surrounding water. Mounting the sensor onto a pressure release surface results in a near-doubling of the incoming acoustic (velocity) signal and produces a directional response, with a resultant improvement in signal-to-electronic-noise ratio. This velocity sensor is not able to respond to signals near  $\theta = 90^\circ$  and  $\theta = 270^\circ$  and has a beam pattern shape similar to half of a dipole. Another advantage of this feature is the rejection of vibrational noise propagating in the plane of the array.<sup>57</sup> The single axis sensor by itself and not mounted on a pressure release baffle would generate a dipole beam pattern. The bimorph flexural disk sensor—even though it measures motion (i.e., velocity) the sensitivity—is often referenced in units of acceleration since it produces a flat response below its resonance. When measured on a shaker table the bimorph flexural disk sensor has an acceleration response shown in figure 44. The bimorph flexural disk sensor has a resonance frequency of 11-kHz and an acceleration sensitivity of  $-17.3 \text{ dB re V/g}$  or  $13.7 \times 10^{-3} \text{ V/(m/s}^2\text{)}$ ,

where  $V$  is the output sensor voltage for 1g unit acceleration applied, 1g is the acceleration of gravity  $9.81 \text{ m/s}^2$ . The farfield acoustic pressure sensitivity can be predicted from acceleration sensitivity using  $M_o = V_{out}/p_{in} = (1/\rho c)(V/u) = (j\omega/\rho c)(V/a)$ , where  $a=j\omega u$  for a plane wave and  $\omega=2\pi f$ . The voltage to acceleration ratio ( $V/a$ ) is the acceleration sensitivity for the bimorph flexural disk sensor. The predicted receive sensitivity is  $-85 \text{ dB re } 1\text{V/Pa}$  and referenced to a  $1 \mu\text{Pa}$  is  $-205 \text{ dB re } 1\text{V}/\mu\text{Pa}$  at 1 kHz.<sup>58 and 59</sup>

Three of these single axis sensors were positioned orthogonal and collocated to one another along the x, y, and z axis with a single pressure sensing hydrophone. Each of the accelerometers provides a dipole response and when combined appropriately with the hydrophone the sensor can form a cardioid beam steerable along each of the axes.<sup>59</sup> The measured frequency response of the hydrophone “P” and two of the accelerometers along the X and Y axis is shown in figure 45. The hydrophone’s response is sufficiently flat within its operating frequency band and its resonance is well above the operating frequency band. Unlike the geophones which have a flat response above its resonance, these have receiving response rises proportionally to frequency  $\omega$  or increases of 6-dB/octave below its resonance. At 1-kHz the measured RVS level is close to what was calculated  $-205 \text{ dB re } 1\text{V}/\mu\text{Pa}$ . The polar response for the X, Y, and Z axis accelerometers and hydrophone P are shown in figure 46 at 1-kHz. All three axis have ideal dipole beam patterns and the hydrophone is onmi-directional.

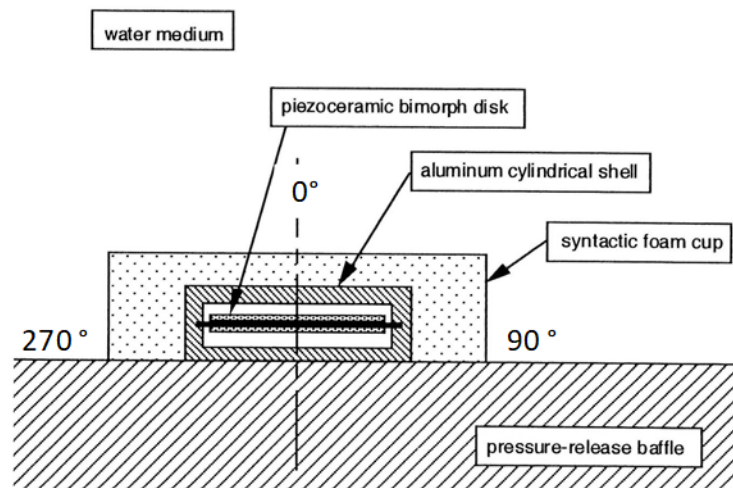


**Figure 43. Single-Axis Acoustic Motion (Velocity) Sensor<sup>57</sup>**

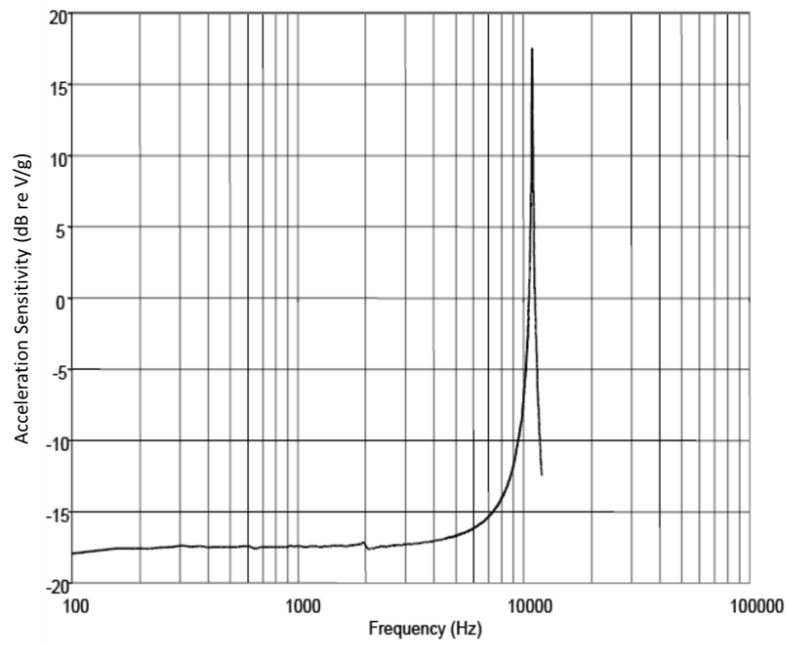


**Figure 44. Flexural Disk Acceleration Sensitivity Response in dB re 1V/g<sup>59</sup>**

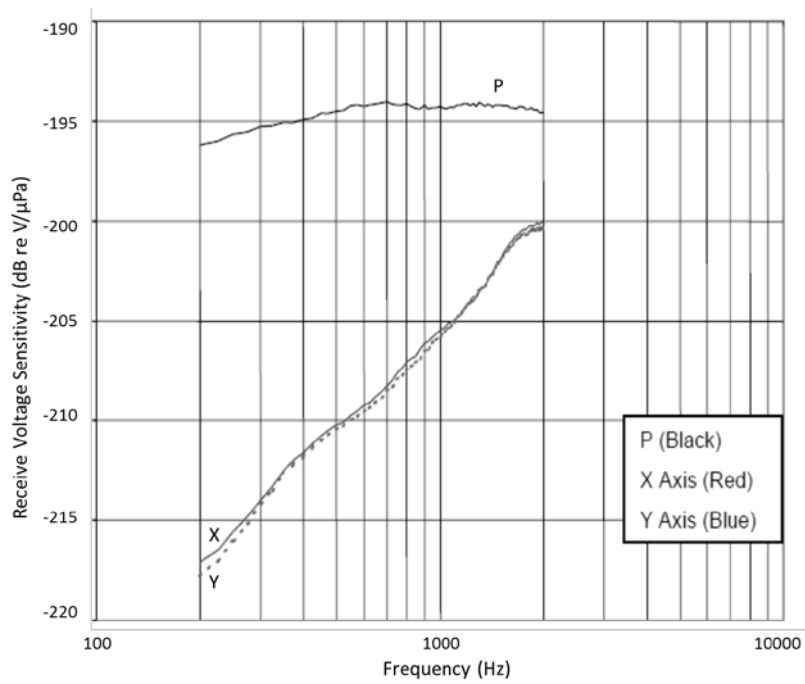


**Figure 45. Measured Receive Sensitivity<sup>59</sup>**

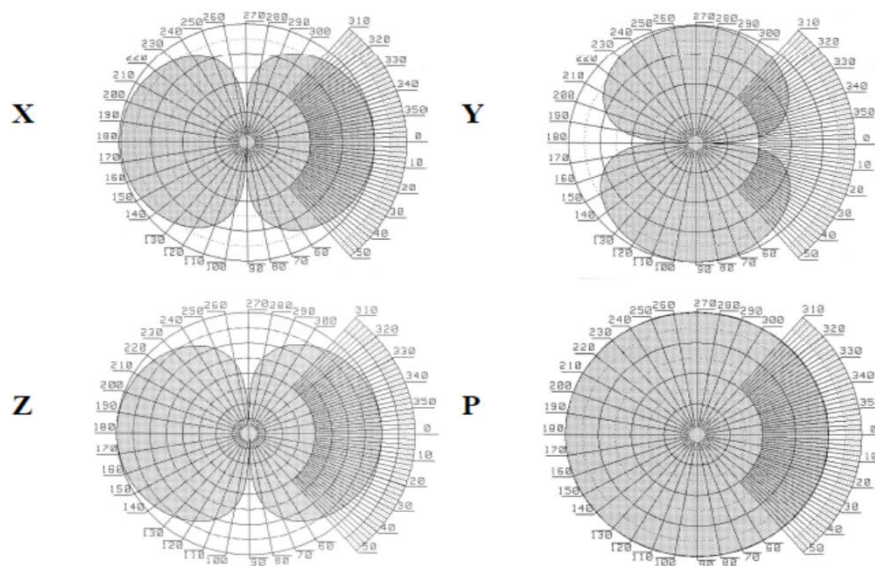


**Figure 46. Measured Beam Patterns at 1-kHz<sup>59</sup>**

Another example of a three-axes acoustic vector sensor is shown in figure 47. This vector sensor is made up of one omnidirectional hydrophone, three orthogonal accelerometers, and a four-channel preamplifier all contained in neutrally buoyant package with a length of 71.3-mm and diameter of 40.7-mm. The accelerometers utilize PMN-PT single crystal material which allowed the vector sensor to be greatly reduced in size to the point where the sensor fits inside existing towed array hoses commonly used by the Navy. The measured frequency response of the hydrophone is shown in figure 48a. The hydrophone's response is sufficiently flat within its operating frequency band and its resonance is well above the operating frequency band. The frequency response of the three accelerometers are shown in figure 48b. The accelerometers exhibit a resonance around 13.5-to-15 kHz. The receiving responses also rise proportionally to frequency  $\omega$  or increases 6-dB/octave below its resonance. The polar response of the hydrophone is shown in figure 49a and is omnidirectional. The polar response for the x and y axis accelerometers are shown in figure 49b and for z axis accelerometer is shown in figure 49c at 7-kHz. All three axis have a classical dipole beam pattern.<sup>60</sup>

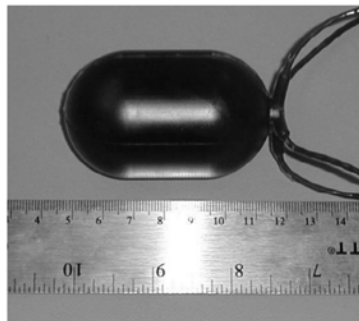
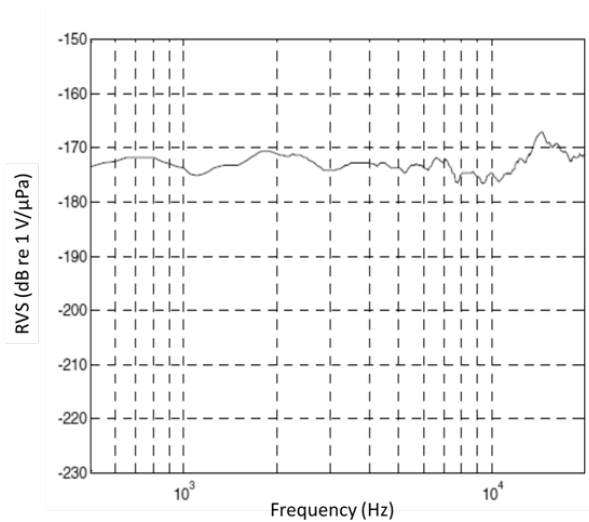
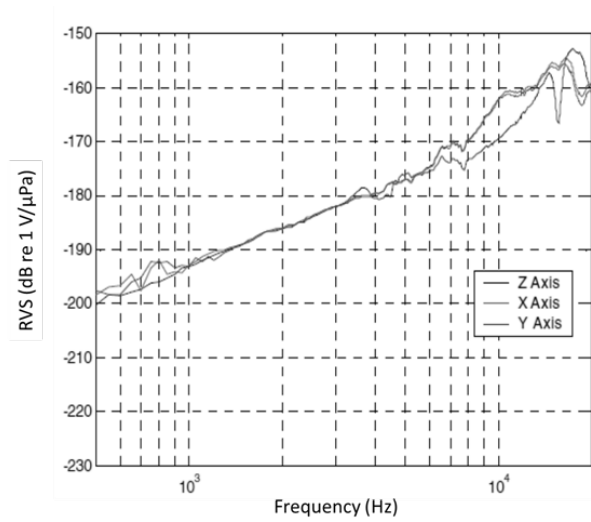


**Figure 47. Wilcoxon Vector Sensor<sup>60</sup>**

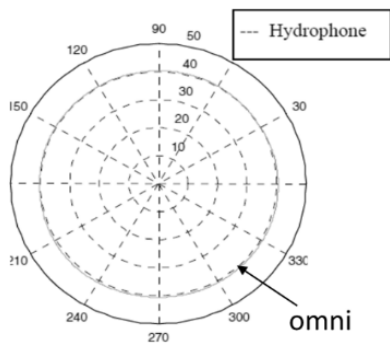


a) hydrophone

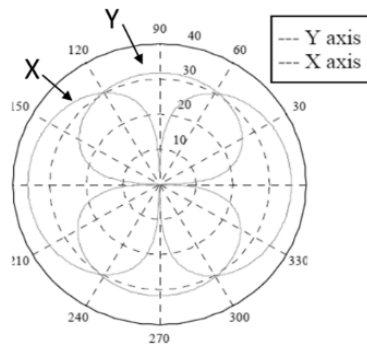


b) X, Y and Z axes

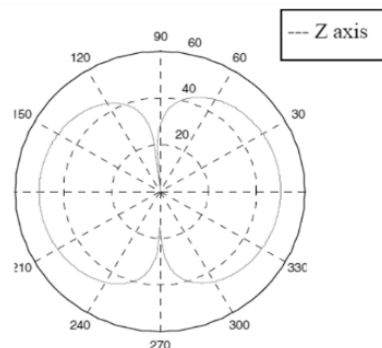
**Figure 48. (a) Hydrophone and (b) Accelerometer RVS Responses Along the X, Y and Z Axis<sup>60</sup>**



a) hydrophone



b) X and Y axis



c) Z axis

**Figure 49. (a) Hydrophone and Accelerometer Beam Patterns Along the (b) X and Y Axis and (c) Z Axis at 7 kHz<sup>60</sup>**

Multimode Hydrophones are built in a similar manner to some omnidirectional hydrophones. The directional response of this type of sensor is due to the piezoceramic elements in a multimode hydrophone being electroded in a fashion that allows the hydrophone to respond to higher-order modes of vibration than those of an omnidirectional hydrophone and can form dipole and cardioid directional beams, as shown in figure 50.<sup>51</sup>

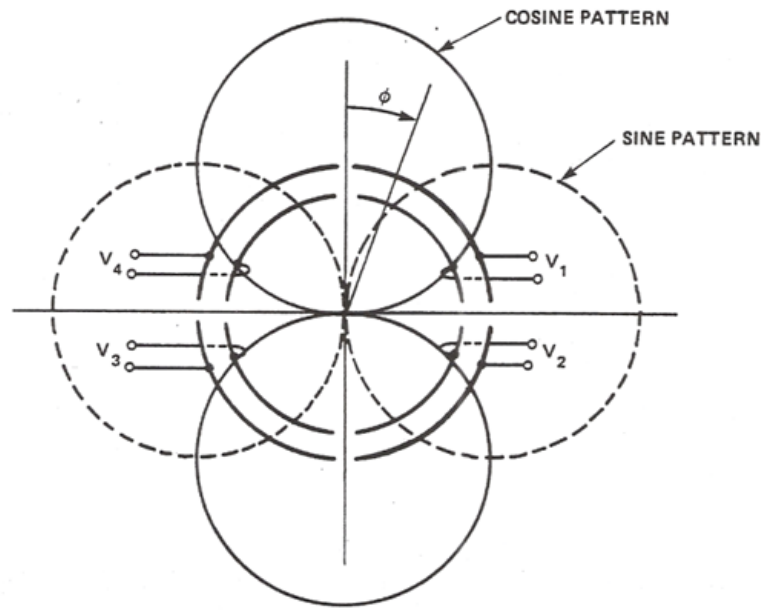
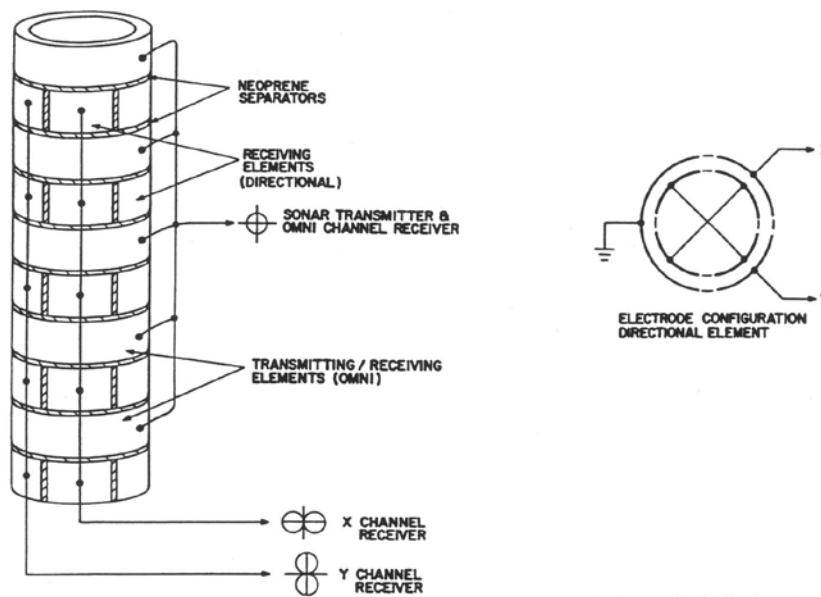


**Figure 50. Multimode Hydrophone Ceramic Cylinders Electroded into Quadrants<sup>51</sup>**

The vertical cylindrical section of the multimode hydrophone is composed of a number of stacked ceramic cylinders with each of the ceramics being electroded into quadrants, as shown in figure 51. By appropriate summing of the signals from the quadrants, three different signals are formed: omni, sine, and cosine. A simple in-phase summing of the four quadrants results in a response pattern that is omnidirectional  $V_{\text{omni}} = V_1 + V_2 + V_3 + V_4$  with respect to azimuth (some vertical directionality exists due to the height of the hydrophone relative to the acoustic wavelength). Summing and differencing operations result in dipole patterns in azimuth. Two sets of patterns, referred to as sine and cosine, are formed using equations  $V_{\text{sin}} = (V_1 + V_2) - (V_3 + V_4)$  and  $V_{\text{cos}} = (V_1 + V_4) - (V_2 + V_3)$ . By comparing the response of the sine and cosine outputs from an acoustic source, the relative bearing to that source can be accurately determined.<sup>51</sup> The example of a multimode hydrophone shown in figure 51 consists of ceramic cylinders used as omnidirectional hydrophones and segmented ceramic cylinders used as pressure gradient hydrophones similar to that used by the Directional Command Activated Sonobuoy System (DICASS) (AN/SSQ-62) Sonobuoy.<sup>53</sup>



Example of Ceramic Cylinders (Multimode ) used as Omni Hydrophones and Segmented Ceramic Cylinders used as Pressure Gradient Hydrophones in an Active / Passive array similar to that Employed by the DICASS (AN/SSQ-62) Sonobuoy

**Figure 51. Multimode Hydrophone Example<sup>53</sup>**

## 2.5 ADVANCED TRANSDUCER TECHNOLOGY

Other advanced transduction technology receiver materials used for hydrophones are the 1-3 Piezo-Composite and Piezo-Rubber composite material shown in figure 52 and PVDF material. The 1-3 piezo-composite material consists of thin piezoceramic PZT rods aligned parallel to the poling direction and imbedded in a polymer matrix (epoxies and polyurethanes). The 1-3 piezo-composite surfaces are coated with copper or silver that act as the electrode. The 1-3 piezo-composite removes lateral lower-frequency modes that are associated solid PZT of the same size in width or diameter; hence, the 1-3 piezo-composite would have a wider receiving frequency response. These are also available in small sheet form and are semi-flexible depending upon the filler matrix material used and are suited to both hydrophones and projectors.<sup>61</sup> The Piezo-Rubber (PZR) are particles of piezoceramics suspended in a rubber-like matrix available in sheets (3.30-mm) thick and are more suited to hydrophone material than to projectors.<sup>62</sup> These materials are available in continuous sheet forms, are semi-flexible, and their surfaces are coated with silver that act as the electrode.

Poly vinylidene fluoride (PVDF) are piezoelectric polymers available in thin sheets (up to 0.50-mm) and are also more suited to hydrophone material than to projectors.<sup>63</sup> The PVDF material has a low-specific acoustic impedance; and therefore, could be used as a transparent hydrophone in front of an existing sonar array. The material is flexible and can be conformally shaped. Its surfaces are coated with copper that act as the electrode which can be etched to form array elements without physically dicing the polymer. The 1-3 Piezo-Composite, Piezo-Rubber composite and PVDF material all exhibit a high-hydrostatic piezoelectric stress constant  $g_h$  and have a moderate dielectric constant (low-capacitance). They are lightweight and can be made

into large flexible sheets at low-cost, which would make them good potential candidates for applications in planar hydrophones for hull-mounted sonar arrays.

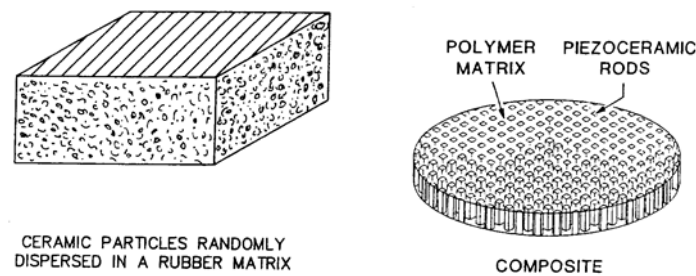


**Figure 52. Configuration of Piezo-Rubber (Left) and 1-3 Composite (Right) Material<sup>61 and 62</sup>**

The fiber-optic sensor is a non-traditional type of hydrophone which uses fiber interferometer techniques, where a fiber-optic coil is wound around a compliant mandrel that is exposed to the acoustic pressure as shown in figure 53, while another identical one is shielded from the acoustic field acting as a reference coil. This makes for a stable sensor unaffected by hydrostatic pressure and temperatures. Figure 54 shows a fiber-optic hydrophone operational schematic using the Mach-Zehnder Interferometer technique where light is passed through the sensing fiber which is modulated by the acoustic pressure field. This phase modulation is then detected interferometrically, by comparing the phase of light in the signal fiber to that in the reference fiber as a phase shift ( $\Delta\phi$ ) per unit acoustic pressure. This phase shift to acoustic pressure ratio is its hydrophone sensitivity in units of  $dB \text{ re rad}/\mu Pa$ . For convenience, since the output of the detector or demodulator output voltage is proportional to  $\Delta\phi$ , then the hydrophone sensitivity can be presented in units of  $dB \text{ re } V/\mu Pa$ . Other fiber-optic hydrophone designs use the Michelson interferometer technique and operate in a similar manner but have mirrors in each of the optical paths which reflect the sensing and reference signal (phase difference) back to the detector.<sup>64</sup> The advantages of the fiber-optic hydrophone are wet-end simplicity, low weight, and reliability. Disadvantages are dry-end cost and complexity.<sup>65</sup>

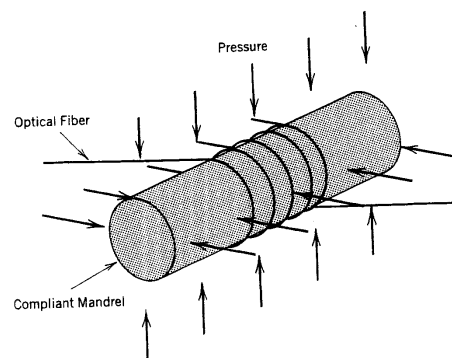


**Figure 53. Mandrel Fiber-Optic Acoustic Sensor<sup>52</sup>**



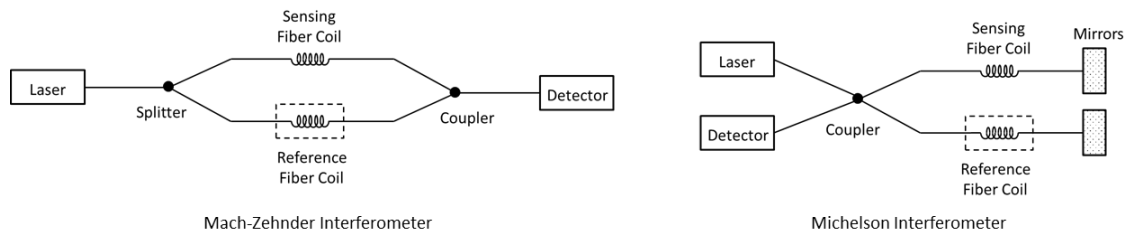


**Figure 54. The Fiber-Optic Interferometer Hydrophone Technique**

### 3. SUMMARY

An overview of transducers that are used for transmitting sound (projectors) and receiving sound (hydrophones) for underwater sonar applications was presented. Transducers are used in all aspects of naval sonar systems on surface ships and submarines for target classification and detection, depth and surface sounding, acoustic communication, homing torpedoes, obstacle avoidance, and alike. The ability to receive and generate underwater sound is based on the science and art of transducer design, which is a specialized science and technology of its own. It includes knowledge of many of the physical sciences such as mechanical, electrical, acoustical, and material sciences. We discussed the most common sonar transducers which are rubber encapsulated electro-mechanical vibrating oscillators with piezoelectric ceramics as the active material. In addition to these basic transducer designs other design types were also discussed. Working design examples were given for both a projector and various hydrophone designs along with an extended list of references.

### 4. REFERENCES

1. B. J. Myers and J. D. Robinson, "Milestones of Innovation: Naval Torpedo Station to Naval Undersea Warfare Center Since 1869," 1<sup>st</sup> edition, published by the Naval Undersea Warfare Center Division, Newport, RI, U. S. Government Printing Office, 2018. (Approved for public release.)
2. Norman Friedman, *The Naval Institute Guide to World Naval Weapon Systems*, 5<sup>th</sup> Ed, Naval Institute Press, Annapolis, MD, 2006.
3. A. D'Amico and R. Pittenger, "A Brief History of Active Sonar," *Aquatic Mammals*, 35(4), 2009, pp. 426–434.
4. J. M. Merrill and L. D. Wyld, *Meeting the Submarine Challenge, A Short History of the Naval Underwater Systems Center*, U. S. Government Printing Office, 1997, p. 68.

5. Thaddeus G. Bell, *Probing The Oceans for Submarines—A History of the AN/SQS-26 Long-Range, Echo-Ranging Sonar*, Peninsula, Los Altos Hills, CA, 2010.
6. R. P. Hodges, “*Underwater Acoustics: Analysis, Design, and Performance of Sonar*,” John Wiley and Sons, Inc., New York, 2011.
7. J. Haystead, “U.S. Navy Enters New era in Undersea Technology,” *Military & Aerospace Electronics Magazine*, Pennwell Publications, April 1994, pp. 20–23.
8. W. M. Jakubowski, “AN/BQG-5A Wide Aperture Array,” *Sea Technology Magazine*, Compass Publications, Inc., November 1996, pp. 43–45.
9. F. V. Hunt, *Electroacoustics-The Analysis of Transduction, and its Historical Background*, Reprint by Acoustical Society of America, Woodbury, NY 1982 originally published in Wiley and Sons, New York 1954.
10. O. B. Wilson, *Introduction to Theory and Design of Sonar Transducers*, 1988 Edition, Peninsula Publishing, Westport CT, 1988.
11. D. Stansfield, *Underwater Electroacoustic Transducers*, 2<sup>nd</sup> edition, Peninsula Publishing, Westport CT, 2017.
12. J. L. Butler and C. H. Sherman, *Transducers and Arrays for Underwater Sound*, 2<sup>nd</sup> edition, ASA Press and Springer, New York, 2016.
13. “Design and Construction of Crystal Transducers,” vol. 12, “Design and Construction of Magnetostrictive Transducers,” vol. 13, National Defense Research Committee (NDRC), Div. 6 Summary, Technical Reports, 1946 (Declassified and Approved for public release.)
14. W. P. Mason, “Piezoelectricity, its History and Application,” *Journal of the Acoustical Society of America*, 70(6), December 1981, pp. 1561–1566.
15. T. F. Hueter, “Twenty Years in Underwater Acoustics: Generation and Reception,” *Journal of the Acoustical Society of America*, vol. 51, no. 3 (part 2), March 1972, pp. 1025–1040.
16. D. Berlincourt, “Piezoelectric Ceramics: Characteristics and Applications,” *Journal of the Acoustical Society of America*, vol. 70, no. 6, December 1981, pp. 1586–1595.
17. Military Standard Mil-Std-1376B, “Piezoelectric Ceramic Material and Measurements Guidelines for Sonar Transducers,” 24 Feb 1995 (Approved for public release.)
18. D. Berlincourt, *Piezoelectric Crystals and Ceramics*, “Ultrasonic Transducer Materials,” ch. 2, edited by O. E. Mattiat, Plenum Press, New York, 1971, pp. 63–124.
19. Leon Camp, *Underwater Acoustics*, John Wiley and Sons, Inc., New York 1970.

20. M. B. Moffett, J. M. Powers, and A. E. Clark, "Comparison of Terfenol-D and PZT-4 power limitations," *Journal of the Acoustical Society of America*, vol. 90, no. 2, Pt. 1, August 1991, pp 1184-1185.
21. A. C. Tims, D. L. Carson, and G. W. Benthien, "Piezoelectric Ceramic Reproducibility (for 33 Mode Transducer Applications)," *IEEE 6<sup>th</sup> International Symposium on Application of Ferroelectrics*, Bethlehem, PA, 8–11 June 1986, pp. 624–627.
22. L. L. Beranek, *Acoustics*, reprint by the Acoustical Society of America, Woodbury, NY 1993, originally published by John Wiley and Sons, New York 1956.
23. J. N. Decarpigny, B. Hamonic, and O. B. Wilson, "The Design of Low-Frequency Underwater Acoustic Projectors: Present Status and Future Trends," *IEEE Journal of Oceanic Engineering*, vol. 16, no. 1, January 1991, pp. 107–122.
24. A. Pierce, *Acoustics*, "An Introduction to its Physical Principles and Applications, Radiation Impedance Curve," *Acoustical Society of America*, Woodbury, New York, 1989, pp 221–225.
25. R. J. Bobbers, *Underwater Electroacoustic Measurements*, 2nd ed., Peninsula Press, Los Altos, CA, 1988.
26. E. Kuntsal, "Free Flooded Ring Transducers," *Oceans 2003 MTS/IEEE: Conference Proceedings*, San Diego, CA, 22–26 Sept 2003.
27. D. F. Jones and J. F. Lindberg, "Recent Transduction Development in Canada and the United States" *Proceedings of the Institute of Acoustics*, vol. 17 part 3, 1995.
28. Ultra Electronics Brochure, "Free Flooded Ring Projector," Ultra Electronics Maritime Systems, Dartmouth, Nova Scotia, Canada, [www.ultra-ms.com](http://www.ultra-ms.com)
29. S. Debost and M. Edouard, "High Power Free-Flooded Ring Transducer," *Proceedings of the Institute of Acoustics*, vol. 21, part 1, 1999.
30. J. B. Lee, "Low-Frequency Resonant-Tube Projector for Underwater Sound," *Proceedings IEEE Oceans' 74*, vol. 2., Nova Scotia, Halifax, 21–23 August, 1974, pp. 10–15.
31. A. L. Butler and J. L. Butler, "A Deep-Submergence, Very Low-Frequency, Broadband, Multiport Transducers," *IEEE Oceans 2002 Conference Proceedings*, Biloxi, MS, see also "Sea Technology," Compass Publications, Inc., November 2003, pp. 31–34.
32. A. K. Morozov and D. C. Webb, "Underwater Tunable Organ-Pipe Sound Source," *Journal of the Acoustical Society of America*, vol. 122, no. 2, August 2007.
33. K. D. Rolt, "The History of the Flexensional Electroacoustic Transducer," *Journal of the Acoustical Society of America*, vol. 87, no. 3, March 1990, pp. 1340–1349.
34. S. C. Butler, A. L. Butler, and J. L. Butler, "Directional Flexensional Transducer," *Journal of the Acoustical Society of America*, vol. 92, no. 5, November 1992, pp. 2977–2979.

35. W. J. Marshall, J. A. Pagliarini and R. P. White “Advances in Flextensional Transducer Design”, *IEEE Oceans*, 1979.
36. B. A. Armstrong and G. W. McMahon, “Discussion of the Finite-Element Modelling and Performance of Ring-Shell Projectors,” *IEE Proceedings*, vol. 131, part F, no. 3, June 1984.
37. R. S. Woollett, “Theory of the Piezoelectric Flexural Disc Transducers with Applications to Underwater Sound,” U.S. Navy Underwater Sound Laboratory, New London, CT, USL Research Report No 490, 5 December 1960. (Approved for public release.)
38. J. Oswin, S. Morgan, and D. Hardie, “Slotted Cylinder Projectors,” *Proceedings of the Institute of Acoustics*, vol. 21, part 1, 1999.
39. G. W. Benthien and S. L. Hobbs, “Modeling of Sonar Transducers and Arrays” Technical Document 3181, SPAWAR Systems Center, San Diego, CA, April 2004. (Approved for public release.)
40. Hydroacoustics Inc., “HVLf-1 Hydroacoustic Low-Frequency Underwater Sound Source Brochure,” Rochester, NY, [www.hydroacousticsinc.com](http://www.hydroacousticsinc.com)
41. J. E. Barger and W. R. Hamblen, “The Air Gun Impulsive Underwater Transducer,” *Journal of the Acoustical Society of America*, vol. 68, no. 4, October 1980.
42. Teledyne Bolt, “Long Life Seismic Source - Brochure, Norwalk, CT, 2015  
[www.teledynemarine.com/bolt/](http://www.teledynemarine.com/bolt/)
43. R. J. Urick, *Principles of Underwater Sound*, 3<sup>rd</sup> edition, Peninsula Publishing, Westport CT 1983.
44. A.D. Jones and P. A. Clarke, “Underwater Sound Received from some Defense Activities in Shallow Ocean Regions,” *Proceedings of Acoustics 2004*, Published by Australian Acoustical Society, Darlinghurst, Australia, 3–5 November 2004.
45. N. R. Chapman, “Source Levels of Shallow Explosive Charges, *Journal of the Acoustical Society of America*, vol. 84, no. 2, August 1988.
46. V. K. Kedrinskii, “Underwater Explosive Sound Sources,” *Encyclopedia of Acoustics*, Ch. 47, edited by M. J. Crocker, John Wiley & Sons, Inc. New York, 1997, pp. 539–547.
47. *USRD Transducer Catalog*, Naval Research Laboratory (NRL) Underwater Sound Reference Detachment (USRD), Orlando, FL, April 1982.
48. T. A. Henriquez, “An Extended-Range Hydrophone for Measuring Ocean Noise,” *Journal of the Acoustical Society of America*, vol. 52, no. 5, November 1972, pp. 1450–1455.
49. R. S. Woollet, “Procedures for Comparing Hydrophone Noise with Minimum water noise,” *Journal of the Acoustical Society of America*, vol. 54, no. 5, November 1973, pp. 1376–1379.

50. T. Straw, "Noise Predicted for Hydrophone/Preamplifier Systems, NUWC-NPT Technical Report-10,369, Naval Undersea Warfare Center Division, Newport, RI, 3 June 1993, (Approved for public release.)
51. C. LeBlanc, "Handbook of Hydrophone Element Design Technology," NUSC Technical Document 5813, Naval Underwater Systems Center, New London, CT, (Now the Naval Undersea Warfare Center Division, Newport, RI), 11 October 1978, (Approved for public release.)
52. R. A. Holler, A. W. Horbach, and J. F. McEachern, *The Ears of Air ASW, A History of the U. S. Navy Sonobouys*, Navmar Applied Sciences Corporation, Warminster, PA, 2008.
53. M. E. Higgins, "DIFAR System Overview," *NUWC/ONR Proceedings of the Workshop on Directional Acoustic Sensors*, Newport, RI, 17–18 April 2001, (Approved for public release.)
54. P. Murphy, "Geophone Design Evolution Related to non-Geophysical Applications," *Acoustic Particle Velocity Sensors: Design, Performance, and Applications*, New York, American Institute of Physics, 1995, pp. 49–56.
55. Geospace Technologies, Houston, TX, [www.geospace.com](http://www.geospace.com)
56. B. M. Abraham, "Low-Cost Dipole Hydrophone for use in Towed Arrays," *Acoustic Particle Velocity Sensors: Design, Performance, and Applications*, New York, American Institute of Physics, 1995, pp. 189–201 and B. M. Abraham and M. J. Berliner, "Directional Hydrophones in Towed Array Systems," *NUWC/ONR Proceedings of the Workshop on Directional Acoustic Sensors*, Newport, RI, 17–18 April 2001. (Approved for public release.)
57. M. Moffett and J. Powers, "A Bimorph Flexural-Disk Accelerometer for Underwater Use," *Acoustic Particle Velocity Sensors: Design, Performance, and Applications*, New York, American Institute of Physics, 1995, pp. 69–83.
58. M. B. Moffett, D. H. Trivett, P. J. Klippel, and P. D. Baird, "A Piezoelectric, Flexural-Disk Neutrally Buoyant, Underwater Accelerometer," *IEEE Trans. Ultrason. Ferroelectric Frequency Control*, vol. 45, no. 5, September 1998, pp. 1341–1346.
59. P. D. Baird, "EDO Directional Acoustic Sensor Technology," *NUWC/ONR Proceedings of the Workshop on Directional Acoustic Sensors*, Newport, RI, 17–18 April 2001, (Approved for public release.)
60. J. Shipps and K. Deng, "A Miniature Vector Sensor for Line Array Applications," *MTS/IEEE Oceans 2003 Proceedings*, vol. 5, 2003, pp. 2367–2370.
61. R. Y. Ting, "New Transduction Materials and their Application in Sonar Transducers," *IEEE, Transducers '91, Digest of Technical Papers, International Conference on Solid-State Sensors and Actuators*, 1991.

62. R. Y. Ting and F. G. Geil, "Recent Development in the Application of 0-3 Piezoelectric Composites for Hydrophone Arrays," *IEEE 7<sup>th</sup> International Symposium on Application of Ferroelectrics*, Urbana-Champaign IL, 6–8 June 1990, pp. 14–17.
63. R.H. Tancrell, D.T. Wilson, N.T. Dionesotes, and L.C. Kupferberg, "PVDF Piezoelectric Polymer: Processing Properties and Hydrophone Applications," *Proceedings of the third International Workshop –Transducers for Sonics and Ultrasonics*, Orlando, FL, 6–8, 1992, Technomic Publishing Company, Inc., Lancaster PA 1993.
64. A. Dandridge, A. B. Tveten, A. M. Yurek, and Y. Y. Chao, "A Fiber Optic Hydrophone for High-frequency Application," *Proceedings of the third International Workshop-Transducers for Sonics and Ultrasonics*, Orlando, FL, 6–8 May 1992, Technomic Publishing Company Inc., Langcaster, PA, 1993.
65. E. Udd, "*Fiber Optic Sensors, An Introduction for Engineers and Scientists*," John Wiley & Sons, New York, 2006.

## INITIAL DISTRIBUTION LIST

Addressee	No. of Copies
Defense Technical Information Center (DTIC)	1
Office of Naval Research (ONR-321MS – M. Wardlaw)	1
Mandex (J. Lindberg)	1
Peninsula Publishing (C. Wiseman)	1
Alan Stuart, Lamont PA	1
Image Acoustics Inc. (J. Butler)	1
Woods Hole Oceanographic Institution (K. Foote)	1
Rite-Solutions (T. Straw)	1